# GEOLOGY OF THE PRECAMBRIAN FARMINGTON COMPLEX, BOUNTIFUL PEAK, MORGAN AND DAVIS COUNTIES, UTAH

A THESIS
SUBMITTED TO THE FACULTY OF THE GRADUATE SCHOOL
OF THE UNIVERSITY OF MINNESOTA

BY
NEIL W. RISMEYER

IN PARTIAL FULFILLMENT OF THE REQUIREMENTS
FOR THE DEGREE OF
MASTER OF SCIENCE

July, 1981

## ABSTRACT

The southern portion of the Precambrian Farmington Canyon Complex is located approximately ten miles north of Salt Lake City, Utah, and forms the westernmost ridge of the Wasatch Mountains overlooking Great Salt Lake. The metamorphic complex consists of complexly deformed, high-grade, biotite-quartz-feldspar gneiss, amphibolite, granitic gneiss, migmatitic gneiss, and pegmatitic granite.

Evidence for at least three episodes of deformation have been observed. Rare evidence for the first event is seen as a refolded isoclinal fold. Northwest trending mineral lineations and folds are a result of the second event. Interference patterns produced by the superposition of two sets of folds suggests a possible, although minor, third deformational event. The last event produced zones of mylonitization, thrust faults, and shear zones, probably during the pre-Late Cretaceous Sevier Orogeny. The preceeding events occurred in the Precambrian.

The Complex has undergone three periods of metamorphism. An Archean granulite facies event has been suggested (Bryant, 1980) but no evidence for this event was observed in this study. Dynamic metamorphism was associated with the Sevier Orogeny.

A middle proterozoic event of upper amphibolite grade, coincident with the second deformational event, attained

P-T conditions up to and possibly above the second sillimanite isograd, as the pelitic assemblage of sillimanite-K feldspar-quartz-muscovite-plagioclase would indicate. The presence of only a few, sparsely located, coarse-grained, leucocratic pods within the laminated biotite-quartz-feldspar gneiss suggests that conditions were not appropriate for broad scale partial melting. Possible explanations for this lack of partial melting include: a) lack of water, b) temperatures too low, or c) anorthite content too high.

## ACKNOWLEDGEMENTS

I wish to thank my advisor, Dr. James A. Grant, who I first met at the Wasatch-Uinta Summer Field Camp. It was at field camp that I was first exposed to the Farmington Canyon Complex.

I would like to thank Dr. Timothy B. Holst and Dr. John C. Green for their helpful suggestions and for serving on my graduate committee. Special thanks goes to Ms. Penney Morton who served as a substitute advisor while Dr. Grant was in England. Her thoughts, suggestions and critisisms were of great help.

Very special thanks must also go to the U.S. Geological Survey for its very generous support of this thesis. Thank you to Richard W. Ojakangas who acted as liaison with the U.S.G.S.

Finally, I want to thank my wife, Wendy, who served as my field assistant and typed this thesis.

# TABLE OF CONTENTS

# ILLUSTRATIONS

## TABLES



## PLATES

# Introduction

## Problem

This thesis concerns the southern portion of the Farmington Canyon Complex as seen along Bountiful Ridge, north of Salt Lake City in the Wasatch Mountains (Figure 1). The Complex consists of various biotite-quartz-feldspar gneisses, amphibolites and pegmatitic granites. At least three episodes of metamorphism have been recognized (Bryant, 1980), with the second event producing the present mineral assemblages and the northwest structural trend. The purpose of this study is to determine the metamorphic and structural history of the Farmington Canyon Complex as seen from field evidence and from detailed petrography.

## Previous Work

Eardley and Hatch (1940) summarized much of the early work on the Farmington Canyon Complex. Captain H. Stansbury first observed the Farmington Mountains in 1849. King, Emmons and Hague explored the Salt Lake area in 1877. Butler, Loughlin and Calkins studied the Precambrian rocks petrographically in 1920. Crawford examined an "Archean" metaquartzite east of Bountiful in 1935. Also in 1935, Blackwelder recognized two divisions in the Precambrian basement rocks of Utah and Wyoming: an Upper Proterozoic "quartzite-slate system" and the underlying middle Precambrian "metaquartzite

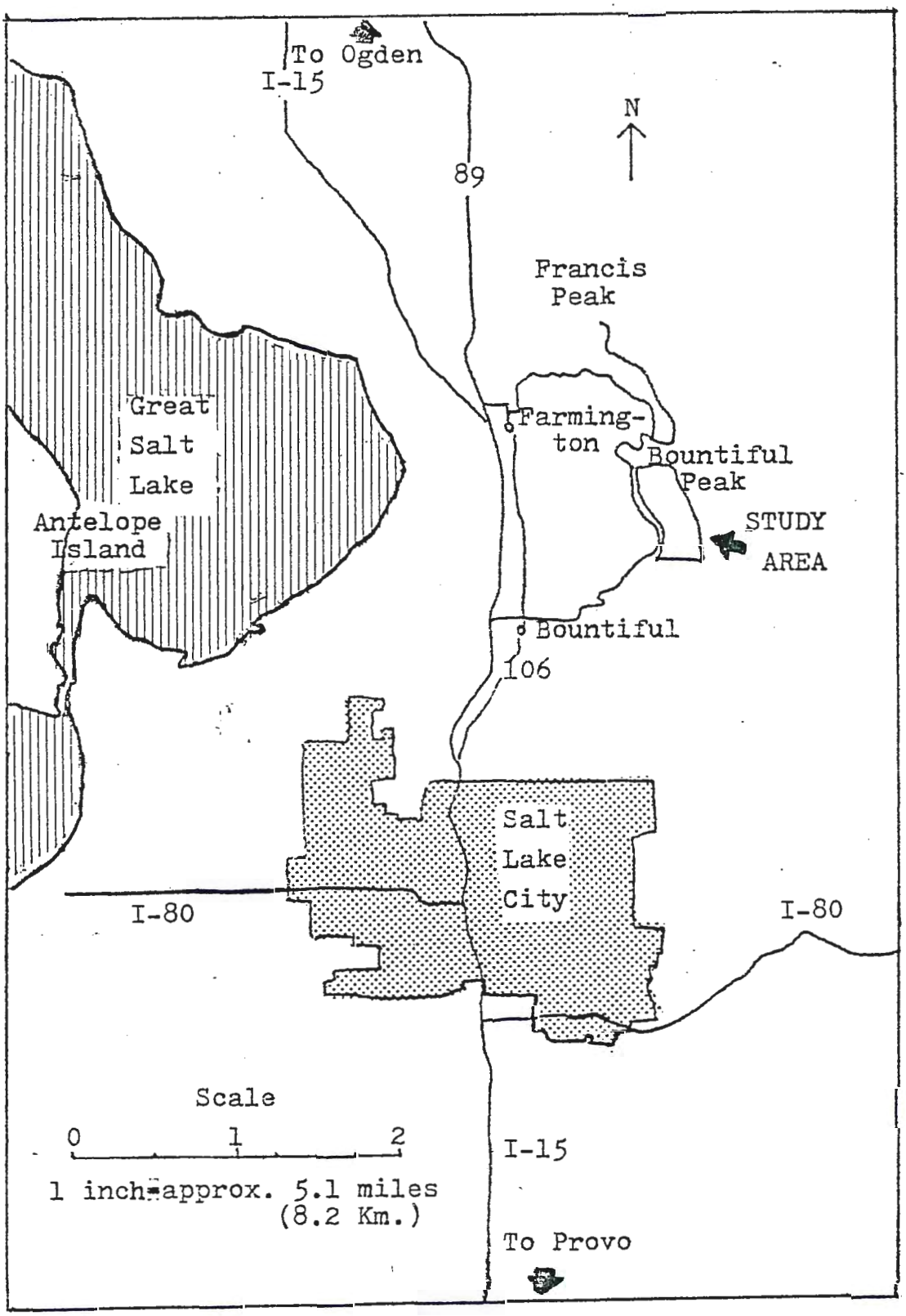


Figure 1: Location Map Of Study Area

and schist system" or what is known today as the Farmington Canyon Complex.

In the late 1930's, Eardley and Hatch studied the stratigraphy, structure and petrography of the Precambrian crystalline rocks of north-central Utah. Bell (1951) discussed the northern half of the Farmington Mountains, from Farmington Canyon, just north of the present study to Weber Canyon at Ogden. Recently, Bryant (1978,1980) studied the metamorphic and structural history of the Farmington Canyon Complex.

Present Study

The specific area studied includes portions of Sections 22, 26, 27, 34, 35 of T. 3 N., R.1 E. and Sections 1, 2, 11, 13 of T. 2 N., R. 1 E. from the Bountiful Peak Quadrangle, Utah. Easy access to the study area is obtained by North Interstate 15 from Salt Lake City to the cities of Bountiful or Farmington. Scenic Skyline Drive, overlooking Great Salt Lake, makes a loop from Farmington upward through Farmington Canyon to Bountiful Peak and then continues on down the Farmington Mountains to the city of Bountiful.

The sharp relief of the Wasatch Front is shown in two adjacent 7.5 minute topographic maps, the Farmington and the Bountiful Peak Quadrangles. The elevation at Farmington Bay is 4205 feet above sea level. Four and one half miles to the east, Bountiful Peak rises abruptly to an elevation of 9259

feet above sea level, nearly one mile above Great Salt Lake.

Field work during the summer of 1980 concentrated on several main objectives:

a) To describe and map the Farmington Canyon Complex along Bountiful Ridge,

b) To determine the metamorphic and structural history there,

c) To determine the relationship of the granitic rocks to the country rocks, and,

d) To investigate the distribution of uranium-thorium in the various rock units of the Farmington Canyon Complex.

The basemap used was the 7.5 minute topographic map of the Bountiful Peak Quadrangle, Utah. The scale was enlarged from 1:24000 to 1:6000. Samples were collected from the different lithologies with special attention given to any textural or mineralogical evidence critical to the metamorphism. Approximately 250 structural measurements were taken and plotted on equal area projections. Thin sections from 120 rocks were studied carefully for textural and mineralogical data pertinent to the metamorphism. Staining of all rock samples for potassium, using sodium cobaltinitrite, and for calcium, using Amarand, aided in determining mineral percentages. The composition of plagioclase was determined by the Michel-Levy method (Kerr, 1977, p. 293).

Uranium-thorium occurrences were detected by the

autoradiography method which utilized photographic film and by the use of a scintillometer in the study area.

General Geology of the Farmington Canyon Complex

Utah's present mountains are the result of uplift and block-faulting which occurred during the last 25 million years (Hintze, 1973). The Farmington Mountains form the westernmost ridge of the Wasatch Mountains, at the eastern border of the Basin and Range Province, extending for 25 miles (40 Km.) between Ogden and Salt Lake City, overlooking the Great Salt Lake valley and separated from it by the Wasatch Fault. (See Figure 2)

The Farmington Canyon Complex (Bryant, 1978) consists of complexly deformed, high-grade, laminated biotite-quartz-feldspar gneisses, amphibolite with varying amounts of quartz, biotite and garnet, granitic gneiss and migmatitic gneisses. In the northern part of the complex, quartz monzonite gneiss containing amphibolite and calc-silicate lenses predominate. Migmatitic gneisses and numerous pegmatitic lenses and stringers also occur. The effects of migmatization decrease south of Farmington Canyon. Near Bountiful Peak, biotite-quartz-feldspar gneiss and pegmatites are abundant. Locally, coarse-grained white quartzite several meters thick, referred to as quartzitic gneiss in this present study, exists south of Bountiful Peak. South of the study area, near Mill Creek, layers of

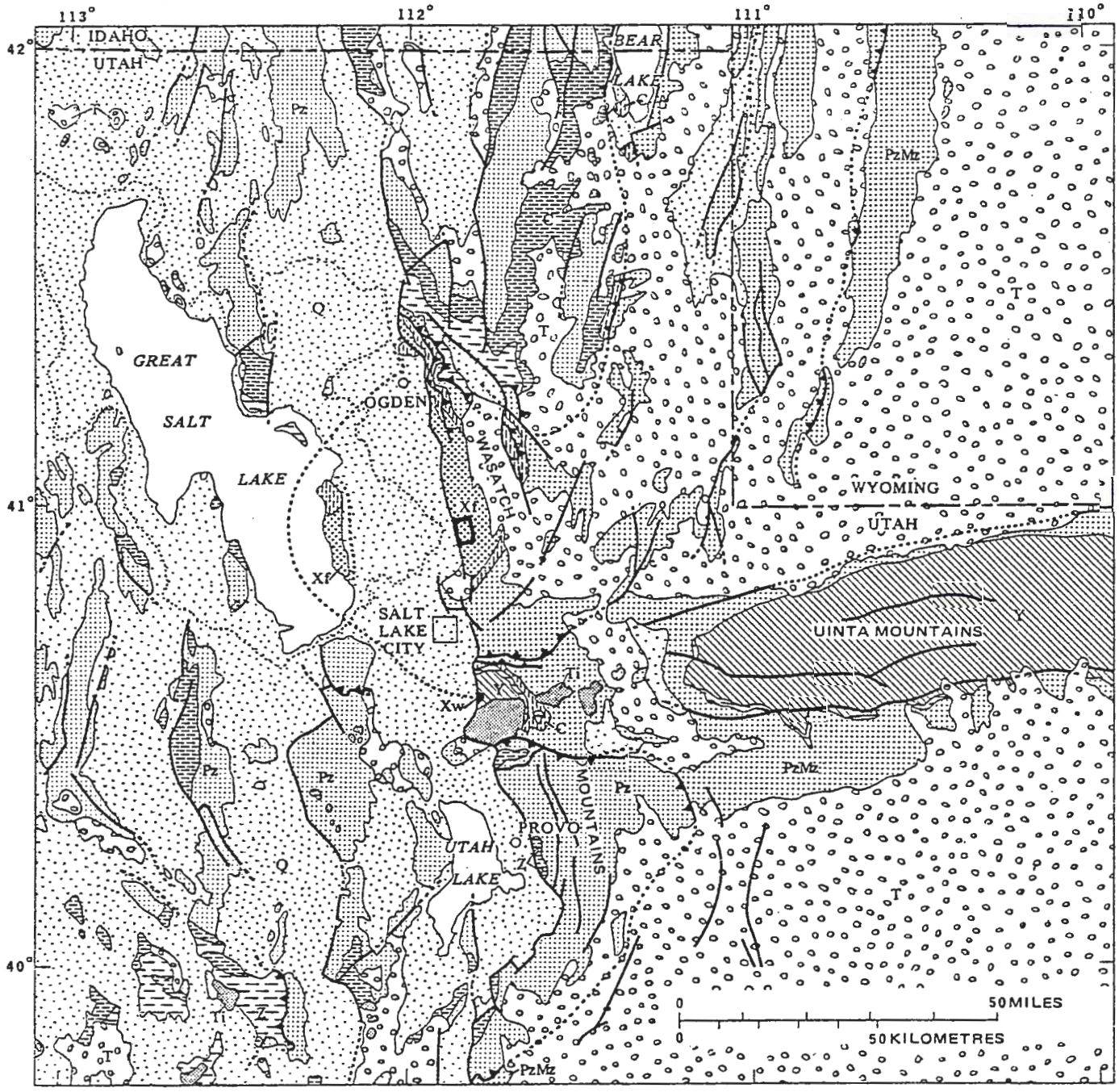


Figure 2: Geologic Map of northeastern Utah.
Study area outlined in center of map.
Q: Quaternary, T: Tertiery, Ti: Tertiery intrusives, Mz: Mesozoic, Pz: Paleozoic, Ꞓ: Cambrian, Precambrian X, Y, Z, Xw: Little Willow Formation, Xf: Farmington Canyon Complex.
(King, 1976)

calc-silicate gneiss are common. Sillimanite is preserved throughout the complex in layers of laminated biotite-quartz-feldspar gneiss. Cordierite-garnet-anthophyllite and cordierite-biotite-sillimanite-garnet assemblages have been recognized southeast of Bountiful Peak.

Evidence for three episodes of metamorphism have been recognized by Bryant(1980). A Late Archean granulite-facies episode may be represented by the presence of relict hypersthene. The second event, of amphibolite-facies, has been dated at 1600-1700 m. y. (Damon and others, 1968) by potassium-argon methods on muscovite (Whelan, 1970). Field observations suggests that the main mineral assemblage of sillimanite, biotite, garnet and microcline in pelitic rocks and hornblende, garnet and biotite in amphibolites was produced during this second event. Also, isoclinal folds with west trending axes and mineral lineations of sillimanite and hornblende paralleling these can be attributed to this event. The third event is characterized by mylonite zones, shear zones and greenschist metamorphism. It affects rocks north of the study area, between Weber and Farmington Canyons (Bell, 1951; Bryant, 1980). Bryant indicates that this cataclastic and retrogressive metamorphism, usually attributed to the Sevier Orogeny (pre-Late Cretaceous, 80 m. y.), may be of Precambrian age.

In the present study, at least three episodes of deformation are observed. The first episode is seen as

refolded isoclinal folds formed prior to the amphibolite-facies metamorphism. The recumbent folds have then been folded. The second fold axis is parallel to the northwest trend of the second metamorphic episode, and therefore may correlate with this metamorphic event (1700 ± 150 m. y.) The last event is represented by highly altered granitic rocks, possibly reflecting shear zones related to the cataclastic and retrogressive metamorphism.

Utah's stratigraphic history can be generalized into six phases of unequal duration as shown in figure 3 (Hintze, 1973). The miogeoclinal phase involved deposition of marine sediments in western Utah. In the Oquirrh and Paradox Basin phase, local deeply subsiding marine basins developed in central and eastern Utah. The Sevier Orogenic phase is characterized by thrust faulting and folding of the former miogeocline in western Utah and by deposition of marine and nonmarine deposits in eastern Utah. The Laramide uplift-Uinta Basin phase marked the end of marine deposition in Utah. Rise of the Uinta Mountains arch, the San Rafael Swell, and the Circle Cliffs and Monument upwarps occurred during this phase. Ignimbrites, lava flows and volcanic breccias formed widespread blankets in western Utah during the Oligocene-Ashflow tuff phase. Uplift and block-faulting during the last 25 million years resulted in a series of north-trending fault blocks in the western half of the state. Nonmarine sediments

and basalts were deposited in the fault-block basins. Lake Bonneville was the latest lake to occupy the fault-block valleys of western Utah.

The Farmington Mountains, including Bountiful Ridge, have been subjected to Pleistocene glaciation. Cirques are well preserved along the east and west sides of the main ridge of the Farmington Mountains.

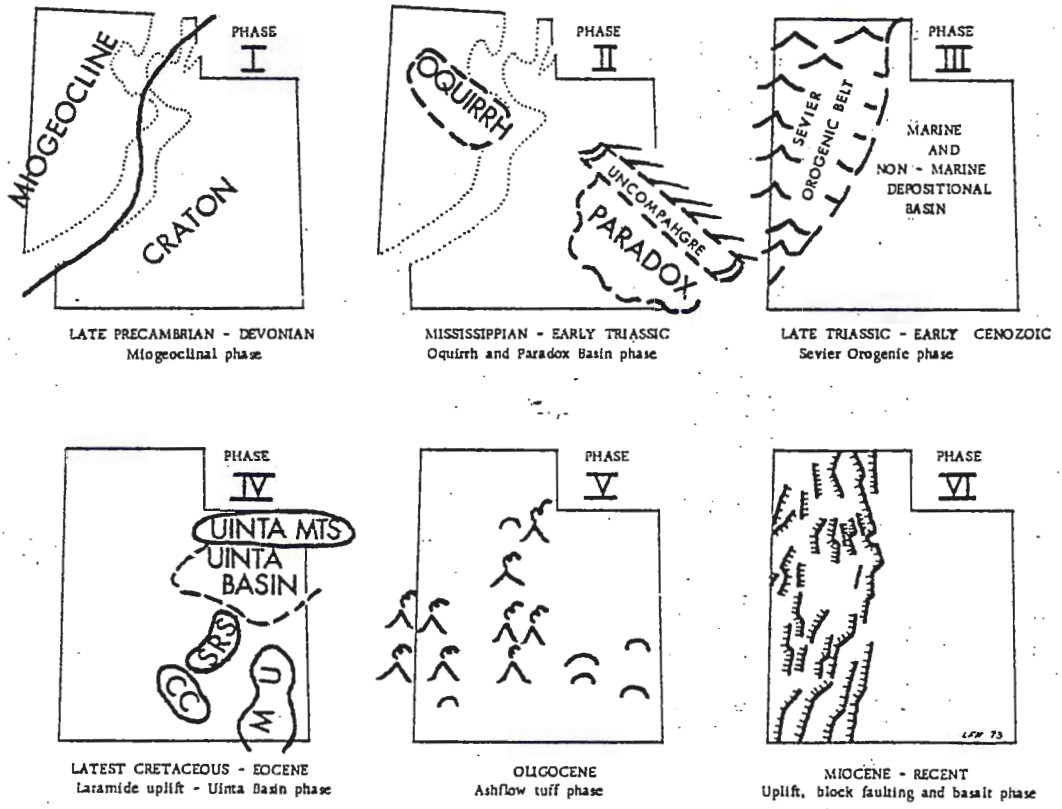


Figure 3: Six phases of Utah's Stratigraphic history. (Hintze, 1973)

## Geology of Bountiful Ridge

The Farmington Canyon Complex consists of a thick sequence of Precambrian metasedimentary and/or metavolcanic rocks, now high-grade gneisses, which have been permeated by granitic and pegmatitic material. To the north and south, the Farmington Complex is overlain directly by basal Cambrian Tintic Quartzite; it is flanked by the Wasatch Fault on the west and Tertiary Knight Formation on the east.

Rock units of the Farmington Canyon Complex are classified under four general headings:

1) Biotite-quartz-feldspar gneisses
   - A) laminated biotite-quartz-feldspar gneiss
     - i) quartzitic gneiss
     - ii) lenticular gneiss
   - B) biotite-sillimanite gneiss
   - C) heterogeneous cordierite-garnet-biotite gneiss

2) Amphibolites
   - A) amphibolite with varying amounts of biotite, quartz and garnet
   - B) migmatitic amphibolite
   - C) garnet augen amphibolitic gneiss

3) Other gneissic rocks
   - A) granitic gneiss
   - B) hornblende-cummingtonite-garnet gneiss
   - C) cordierite-garnet-anthophyllite gneiss

4) Granites
   - A) pegmatitic granite
   - B) sheared granite

## Biotite-quartz-feldspar gneisses

### Laminated biotite-quartz-feldspar gneiss

Tan-to-gray, fine-to-medium grained, lineated, laminated biotite-quartz-feldspar gneiss is the most extensive gneissic unit exposed along Bountiful Ridge. It is well exposed at Bountiful Peak and further south as isolated rafts (15 to 30 meters thick) in pegmatitic granite (e.g. N. ½ of section 2 and S. ½ of section 12, Plate 1). The foliation within these isolated rafts appears to parallel the trend of the regional foliation, indicating there was little or no apparent rotation during emplacement of the granite.

Within this unit are thin horizons, or beds, of quartzitic gneiss and lenticular gneiss. Pale-green, quartzo-feldspathic gneiss, mapped in the field as quartzitic gneiss, is closely associated with shear zones on the flanks of Bountiful Peak. Petrographically, it is texturally and mineralogically equivalent to the laminated biotite-quartz-feldspar gneiss except that it is represented on Plate 1 as altered laminated biotite-quartz-feldspar gneiss.

Compositional layering is defined by alternating light and dark bands of quartz-plagioclase-microcline (1-10 mm wide) and biotite-quartz (1-2 mm wide), respectively. Axial planar foliation is defined by convergent fans of linear, blue-green, quartz-muscovite-sillimanite knots that are disseminated throughout the unit (figure 4). Biotite is generally parallel

to the compositional layering so that it wraps around the hinges of simple open folds but minor amounts of biotite are also recrystallized parallel to the axial planes of the same open folds.

Laminated biotite-quartz-feldspar gneiss is composed of equigranular (1 mm) quartz (47-54 %), microcline perthite (22-28 %), plagioclase (10-15 %, $An_{34-45}$), biotite (4-15 %). garnet (0-6 %), muscovite (1 %), sillimanite and accessory magnetite, apatite, epidote and zircon.

Leucocratic bands consist of an equigranular, mosaic of interlocking quartz, plagioclase and potassium feldspar. Quartz is slightly elongate with irregular grain boundaries and is interstitial to feldspar. Microcline is perthitic and xenomorphic. Plagioclase is typically intergrown with quartz forming myrmekite. Minor biotite and accessory apatite and zircon are present.

Biotite-rich bands are characterized by a wavy, discontinuous foliation of decussate clots of biotite. Trace amounts of muscovite are intergrown with biotite. Very fine-grained, interlocking, strained quartz is disseminated within the biotite foliation.

Linear, waxy, green quartz-muscovite-sillimanite knots (15 x 2.5 x 1 cm) are common throughout the laminated biotite-quartz-feldspar gneiss. Their trend is parallel to major northwest fold axes (see structure chapter). Texturally, the knots are composed of swirling, fibrous mats of fine-grained

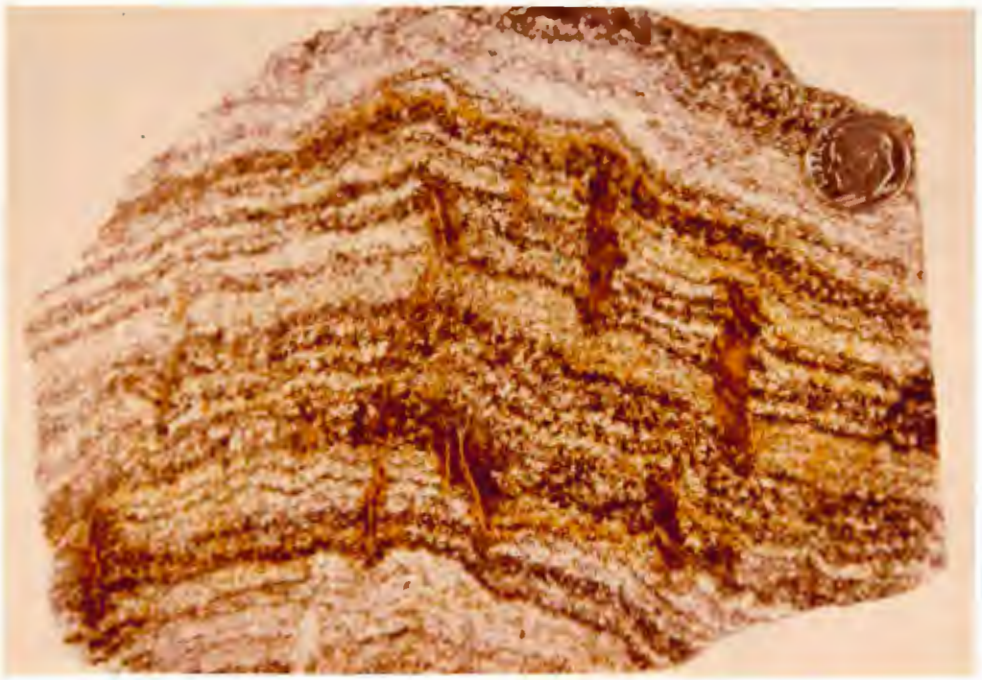

Figure 4: Hand sample of laminated biotite-quartz-feldspar gneiss. Note axial planar foliation of quartz-muscovite-sillimanite knots. Location 28.

sericite plus needles and prisms of sillimanite which penetrate elongate quartz grains (figure 5). No potassium feldspar is present in these knots.

However, potassium feldspar does coexist with sillimanite in some quartzo-feldspathic bands, where sillimanite needles and prisms penetrate microcline. Sillimanite and microcline are associated with quartz, muscovite and biotite (figure 6).

Thin leucocratic pods and lenses, found sporadically within the gneiss unit, are characterized by coarser grain size of quartz and potassium feldspar and by only trace amounts of plagioclase. One such pod consists of hypidiomorphic microcline (3 mm - 2 cm, 55 %), interstitial quartz (2-10 mm, 38 %), xenomorphic, partially saussuritized plagioclase 91 mm, 1 %), interstitial muscovite (1-7 mm, 6 %) and a trace of biotite. Broken microcline grains, in optical continuity, are enclosed by single grains of muscovite (figure 7).

Another lens of coarse-grained quartz and potassium feldspar with penetrating sillimanite prisms and needles was observed (figure 8). The outer edge consists of a fibrous mat of sericite-sillimanite, and biotite enclosing sillimanite prisms, all enclosing garnet porphyroblasts (3-6 mm) (figure 9). The garnet is partially surrounded by sericite and sillimanite, but also by a thin rind of microcline. The microcline appears to be in optical con-

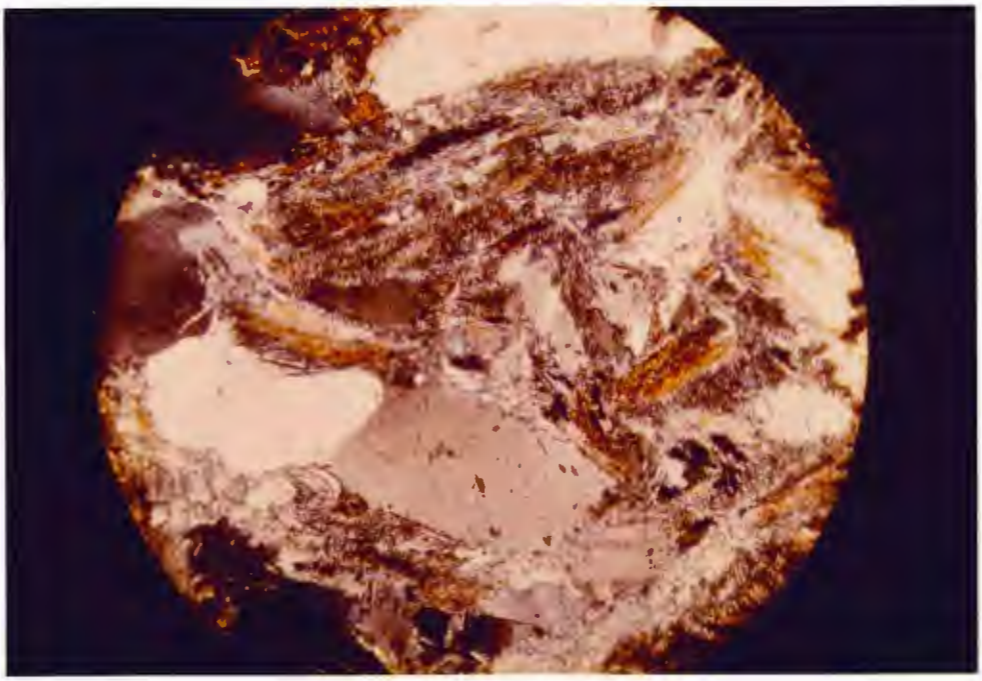

Figure 5: Quartz-muscovite-sillimanite knot occurs as swirling, fibrous mats within laminated biotite-quartz-feldspar gneiss. Field of view: 1.25 mm. X-nicols. FCB 5-15.

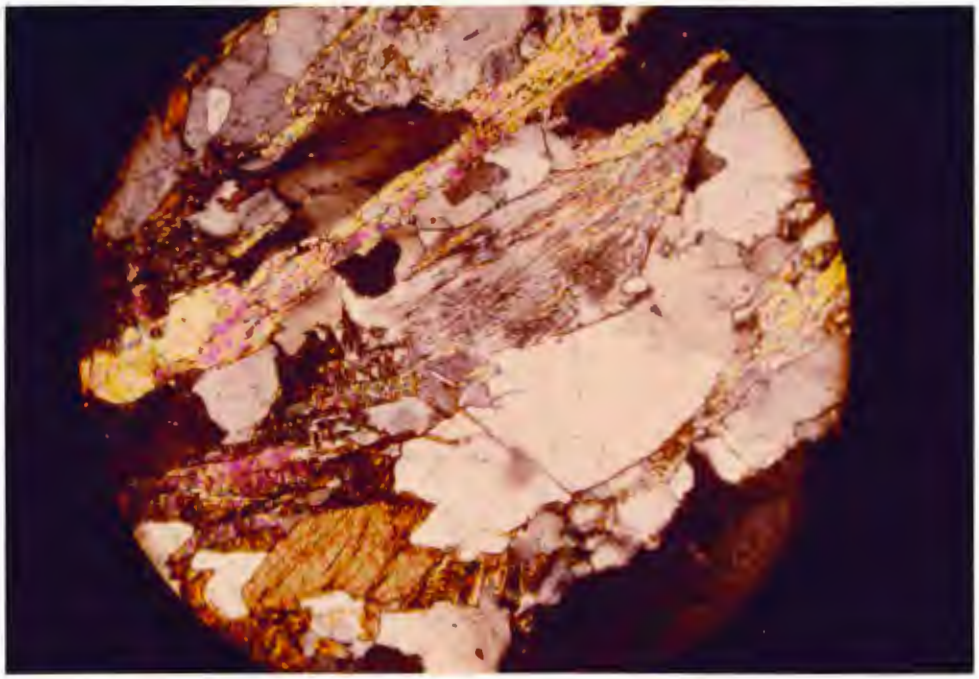

Figure 6: Second sillimanite isograd. Breakdown of quartz + muscovite = K-feldspar + aluminosilicate + $H_2O$. sillimanite occurs as needles in microcline. Field of view: 1.25 mm. X-nicols. FCB 5-13.

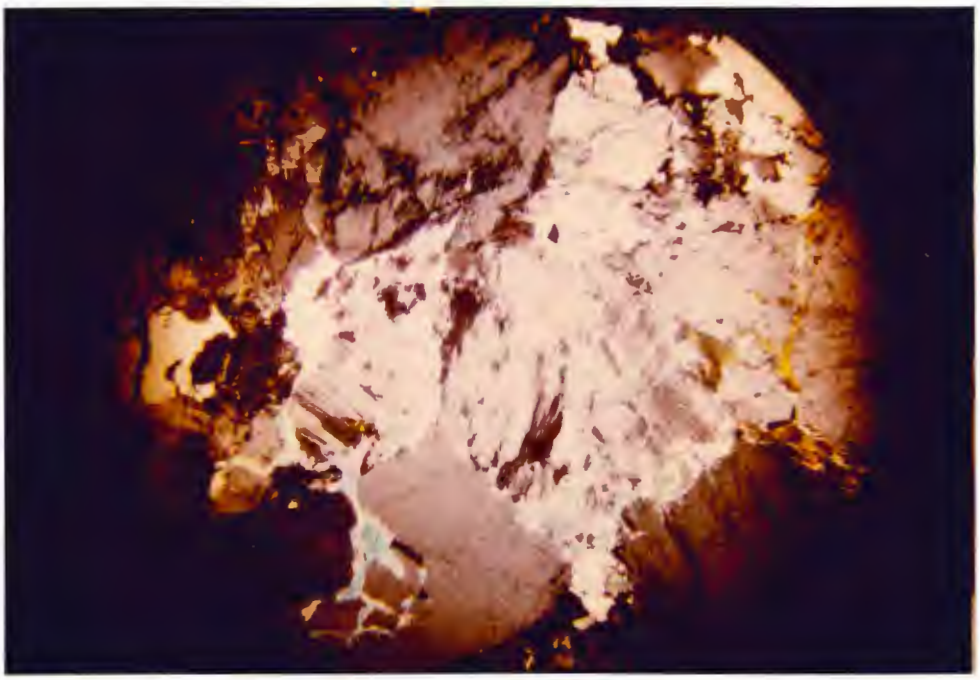

Figure 7: Leucocratic pod within laminated biotite-quartz-feldspar gneiss. Large grains of muscovite enclose broken grains of microcline (in optical continuity). Field of view: 13 mm. X-nicols. FCB 69.

Figure 8: Hand sample of leucocratic lense within laminated biotite-quartz-feldspar gneiss. FCB 5-15.

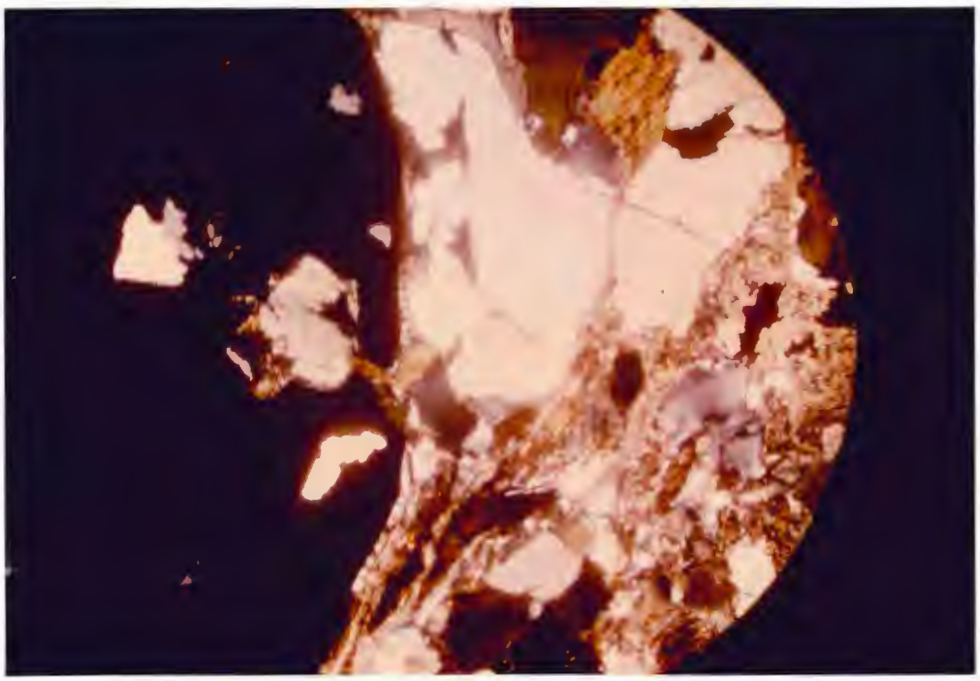

Figure 9: Garnet porphyroblast rimmed by thin rind of microcline. Note microcline also forms thin rind within embayment.
Field of view: 1.25 mm. X-nicols. FCB 5-15.

tinuity, suggesting the rind consists of one grain of microcline. Quartz has sutured grain boundaries and contains penetrating needles of sillimanite.

Important mineral assemblages include:

- K-feldspar-garnet-biotite
- K-feldspar-sillimanite-biotite

plus plagioclase-quartz-muscovite.

Quartzitic gneiss

Gray, medium-grained, sparsely laminated, quartzitic gneiss is exposed locally within the laminated biotite-quartz-feldspar gneiss in the N. $\frac{1}{2}$ of section 2. It is composed of an interlocking mosaic of inequigranular quartz (90-95 %, 1-4 mm), microcline perthite (1-3 %, 1 mm), saussuritized plagioclase (1-2 %, 1 mm), biotite (1 %, 1 mm), muscovite (1 %, 1 mm), accessory epidote, rutile, sphene and zircon. Grains are irregular and have sutured boundaries.

Mineral assemblages in the quartzitic gneiss include:

- K-feldspar-plagioclase-quartz-muscovite
- Biotite-plagioclase-quartz- muscovite

Lenticular gneiss

Black, fine-to-medium grained, lineated biotite-quartz-feldspar lenticular gneiss is exposed in the S.W. $\frac{1}{4}$ of section 26, approximately 600 meters (2000 feet) southeast of Bountiful Peak (Plate 1), but can also be observed as three foot thick horizons within laminated biotite-quartz-feldspar gneiss (e.g. Location 28, Plate 1). These thin horizons of lenticular gneiss cannot be traced from one locality to the next due to the structural complexity of the Farmington Canyon Complex.

This rock unit is characterized by a lenticular banding of elongate quartzo-feldspathic pods (15 x 4 x 1 cm). These pods, which are matrix supported, are of three compositions: 1) white, medium-to-coarse grained quartz-rich (granitic) pods, 2) white, fine-to-medium grained quartz-plagioclase (granitic) pods, and 3) gray, fine-grained biotite-quartz-plagioclase (gneissic) pods. The white granitic pods have convex shapes, whereas the gneissic type pod is elliptical. The matrix is composed of fine-grained, foliated biotite (45-50 %), plagioclase (20-25 %, $An_{40}$), quartz (20-25 %), minor euhedral garnet (1-2 %), accessory zircon, apatite, epidote and rutile. Biotite is slightly replaced by chlorite, and is sometimes kinked. Plagioclase is partially altered to sericite, and quartz is slightly strained. Epidote and chlorite are secondary minerals.

The medium-to-coarse grained quartz-rich pods consist of an interlocking network of slightly strained quartz (3-7 mm. 59 %), and anhedral, partially altered plagioclase (1-4 mm, 38 %, $An_{44}$), and biotite (1-2 mm, 3 %). Plagioclase is poikilitic containing rounded inclusions of quartz.

Fine-to-medium grained quartz-plagioclase pods differ mainly in grain size form the coarse-grained, quartz-rich pods. They consist of an interlocking network of slightly altered plagioclase (1-3 mm, 50 %, $An_{42}$), quartz (1-2 mm, 47%), biotite (1-2 mm, 2 %) and minor euhedral garnet (1 mm, 1 %).

The gray, fine-grained gneissic biotite-quartz-plagioclase pods display a simple schistosity due to preferred orientation of biotite. They consist of fine-grained (1-2 mm) quartz (44 %), plagioclase (44 %, $An_{40}$), biotite (12 %), minor garnet, apatite, rutile and zirçon.

Important mineral assemblages include:

- garnet-plagioclase-quartz
- garnet-plagioclase-biotite-quartz
- plagioclase-biotite-quartz

Biotite-sillimanite gneiss

Biotite-sillimanite gneiss occurs as small lenticular units within amphibolite in S. ½ of section 35, and in laminated biotite-quartz-feldspar gneiss and granite in S. ½ of section 12. It is characteristically rusty-brown, greasy, well foliated and fine-to-medium grained.

Biotite-sillimanite gneiss is composed of equigranular (1-2 mm) brown biotite (20-50 %), quartz (10-25 %), xenomorphic plagioclase (10-20 %), sillimanite (5-15 %), sericite and fine grained muscovite (0-5 %), a trace of garnet, and accessory apatite, rutile and zircon. Sillimanite occurs as fibrolite, prisms and needles and usually occurs intergrown with biotite. Garnet is elongate and highly fractured. Quartz occurs in quartz-feldspar stringers, and as elongate, polycrystalline rods. Sericite replaces quartz along fractures. Foliation consists of a swirling matted felt of biotite, sillimanite plus sericite and/or muscovite surrounding quartz-feldspar lenses.

Pertinent mineral assemblages include:

- biotite-sillimanite
- biotite-garnet

plus quartz and plagioclase.

Heterogeneous cordierite-garnet-biotite gneiss

Cordierite-garnet-biotite gneiss is gray porphyroblastic and medium-grained with a wavy foliation defined by alternating quartzo-feldspathic and mafic-rich bands. It is exposed in the N. W. ¼ of section 35 (location 29), in the S. W. ¼ of section 1 (location 50 and 63) and along Skyline Drive in section 2 (location 53). Migmatitic amphibolite and cordierite-garnet-anthophyllite gneiss are associated with cordierite-garnet-biotite gneiss (location 29). Elsewhere, it is associated with cordierite-garnet-biotite gneiss (locations 50, 53, and 63).

Cordierite-garnet-biotite gneiss consists of cordierite (10-30 %), garnet (5-10 %), biotite (1-3 mm, 20-30 %), plagioclase (1-2 mm, 15-20 %, $An_{30-40}$), quartz (1-2 mm, 10-15 %), sillimanite (0-2 %), accessory apatite, magnetite, zircon and secondary epidote and sericite.

Mafic-rich bands, consisting of foliated biotite, cordierite, garnet, plus sillimanite, alternate with bands of granoblasitc, xenomorphic plagioclase and interstitial quartz. Cordierite is faint blue on fresh surfaces and pale green on weathered surfaces (figure 10). It is confined within the mafic bands and is associated with biotite, garnet and sillimanite (figures 11 and 12). It occurs as coarse-grained

Figure 10: Hand samples of cordierite-garnet-biotite-gneiss exhibiting porphyroblastic texture and wavy foliation. Cordierite alters green on weathered surfaces. Large cordierite porphyroblast is 2 cm. across. Location 29

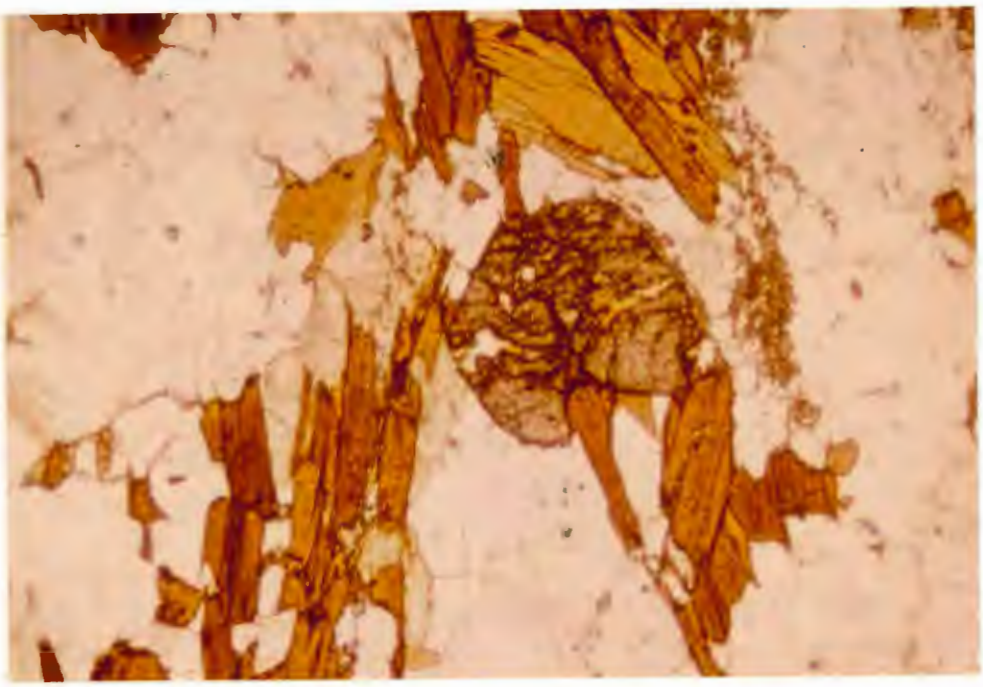

Figure 11: Cordierite-garnet-biotite gneiss. Foliation of mafic bands defined by biotite, garnet, cordierite and sillimanite. Cordierite is light yellow mineral intergrown with biotite. Field of view: 2.5 mm. Plain light. FCB 53.

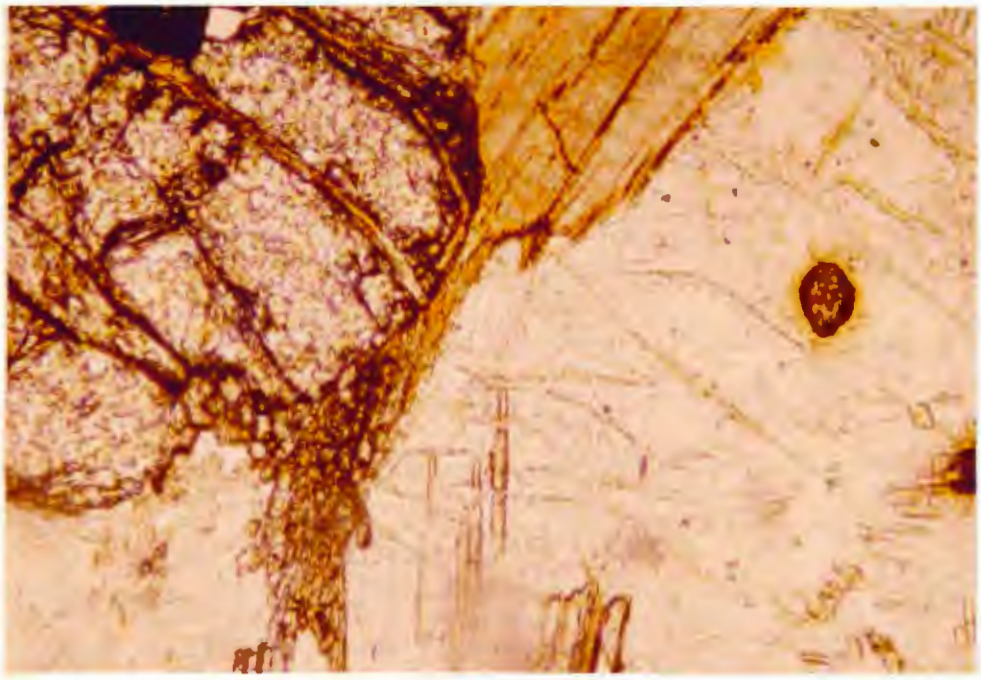

Figure 12: Cordierite-garnet-biotite gneiss. Four phase assemblage of cordierite-garnet-biotite-sillimanite. Yellow pleochroic halo about included zircon within cordierite (Also see Figure 29).
Field of view: 0.6 mm. Plain light. FCB 53

porphyroblasts and as xenomorphic masses enclosing foliated biotite. Pinite alteration is diagnostic. Coarse, radiating prisms of sillimanite occur within the porphyroblasts (figure 13).

The garnet (1-3 mm) in the mafic bands is slightly poikiloblastic and generally idiomorphic, but xenomorphic grains are also present. Foliated biotite and prismatic sillimanite enclose garnet (figure 11). Xenomorphic cordierite also commonly encloses garnet.

As previously noted, sillimanite occurs in two habits: 1) coarse prisms in cordierite, and 2) prismatic cross-sections that occur in close association with cordierite and biotite, but are also found within the quartzo-feldspathic segregations. Rhombs parallel biotite foliation within xenomorphic cordierite.

A migmatitic zone (5-10 meters wide) within this unit is characterized by leucocratic stringers which parallel the foliation and exhibit pinch and swell and boudinage structures (figure 14) and by highly contorted and folded leucosomes one half meter wide (figure 15). The leucosomes consist of coarse-grained (5-10 mm) granoblastic quartz (60-65 %) and untwinned plagioclase (35-40 %, $An_{15-20}$). Some highly altered, green, cordierite grains (2-5 mm) are present in the leucosome (figure 16). A thin selvage of biotite borders the leucosome.

The melanosome consists of fine-grained, equigranular, granoblastic quartz and plagioclase ($An_{30-40}$) and fine-grained

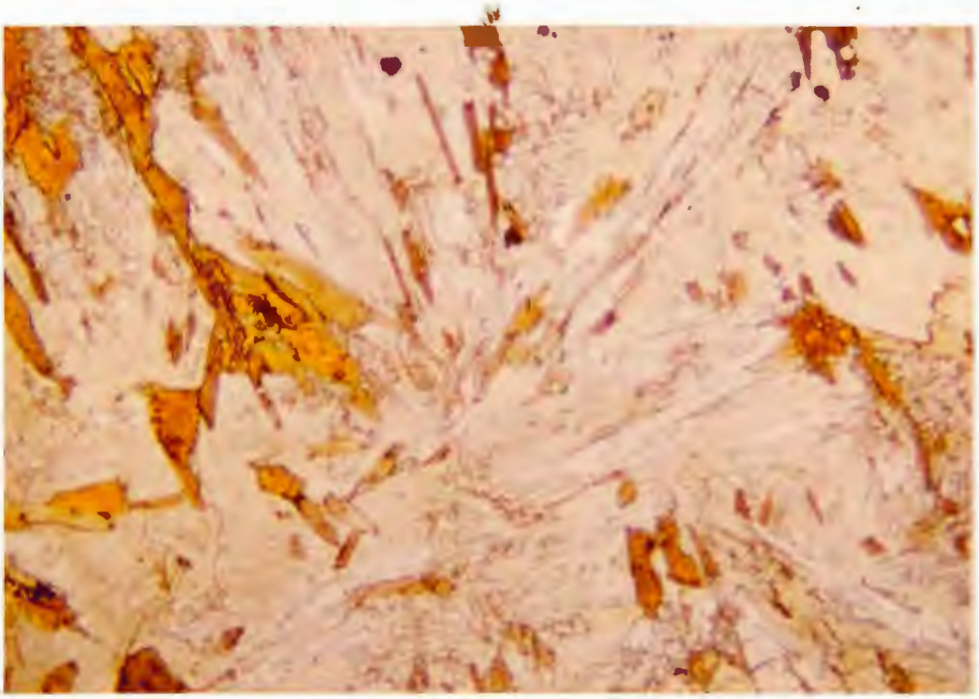

Figure 13: Cordierite-garnet-biotite gneiss. Cordierite porphyroblast with radiating prisms of sillimanite and biotite.
Field of view: 6 mm. Plain light. FCB 29a.

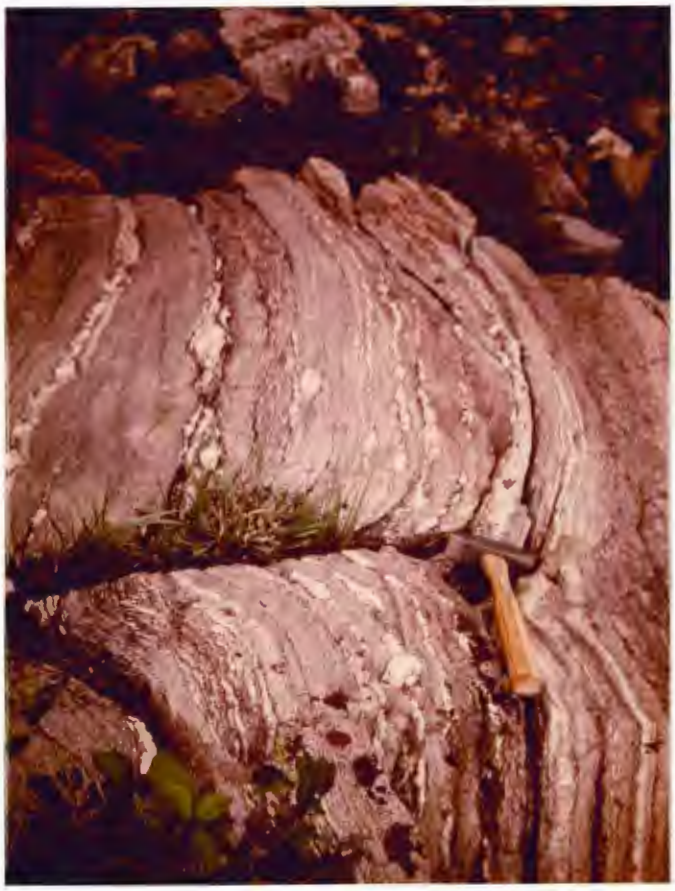

Figure 14: Migmatitic zone within the cordierite-garnet-biotite gneiss. Leucocratic stringers parallel to the foliation exhibit pinch and swell and boudinage structures. Location 29.

Figure 15: Migmatitic zone within the cordierite-garnet-biotite gneiss. Highly contorted and folded leucosome. Location 29.

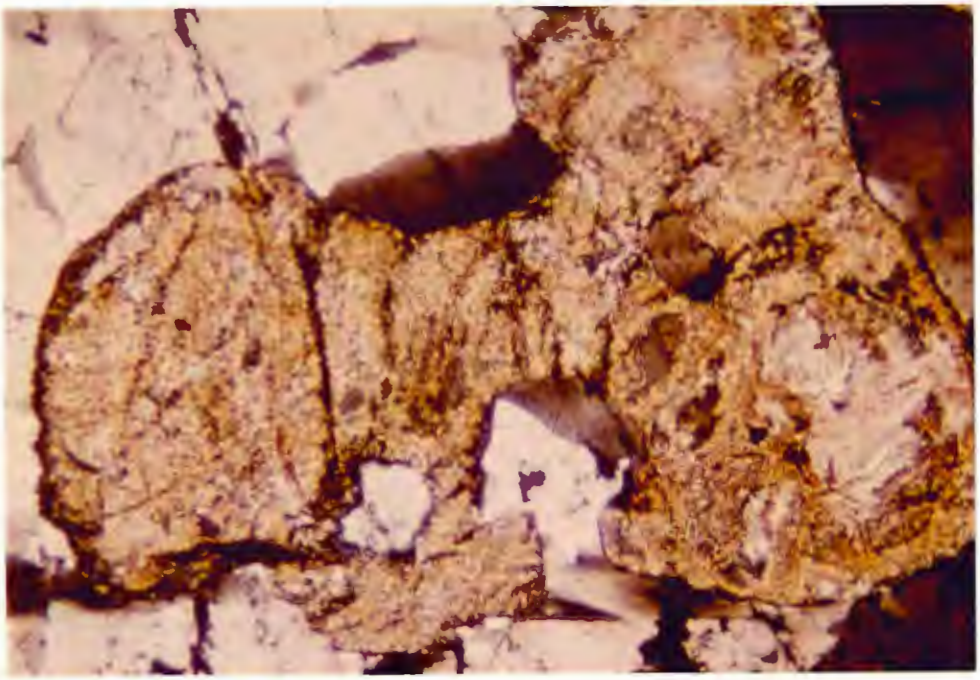

Figure 16: Highly altered cordierite found in the leucosome of figure 15.
Field of view: 6 mm. X-nicols. FCB 29g-2.

biotite, with preferred orientation that defines a simple gneissic layering. Minor garnet, but no cordierite was observed.

Pertinent mineral assemblages include:

- biotite-sillimanite-cordierite
- biotite-garnet-cordierite
- biotite-garnet-sillimanite
- garnet-sillimanite-cordierite
- garnet-sillimanite-cordierite-biotite

plus quartz, plagioclase and magnetite.

## Amphibolites

### Amphibolite

Dark green to black, fine-to-medium grained amphibolite is exposed along Bountiful Ridge as lenticular units varying in size from small (about 1 meter wide) lenses to large lensoidal units (30-250 meters wide by several hundred meters long) which appear to be interlayered with the other gneissic units. Amphibolite is readily distinguished from quartzo-feldspathic gneiss by its color and occurrence as large, flat, tabular slabs.

Sharp contacts are present where a small amphibolite lens pinches out into the laminated biotite-quartz-feldspar gneiss (figure 17). Gradational contacts are also observed over a one meter zone where amphibolite is in contact with granitic gneiss (location 60, Plate 1). Quartz, which has undergone slight to moderate recrystallization, and plagioclase segregations define a moderate foliation where the

Figure 17: Thin lense of amphibolite pinching out into laminated biotite-quartz-feldspar gneiss. Book is resting on amphibolite. Location 28.

amphibolite is in contact with the pegmatitic granite (location 12, Plate 1).

Lithologic variation within amphibolite is common, expressed by differences in the relative amounts of biotite and quartz. Hornblende and biotite together form a well defined foliation. Hornblende also defines a crude lineation parallel to the major northwest structural trend of the area.

The amphibolite consists of hornblende (48-61 %, 2-4 mm), cummingtonite (4 %, 2-4 mm), plagioclase (25-30 %, 2 mm), quartz (7-30 %, 2 mm), biotite (0-8 %, 2-4 mm) and epidote (0-17 %). Accessory minerals include opaques (probably ilmenite), garnet, apatite and zircon.

Hornblende is prismatic and exhibits a crude dimentional preferred orientation occurring in two habits: 1) finer-grained (2 mm) prisms, and 2) as subhedral, coarser-grained (2-4 mm) crystals forming decussate-granoblastic clots up to 8 mm in size. Rounded quartz and plagioclase occur as inclusions within hornblende.

Plagioclase ($An_{53}$) is fine-grained and nearly completely saussuritized in the amphibolite. Small, rounded inclusions of quartz are common.

The amount of biotite varies, but where present, it defines a planar foliation in the amphibolite. It occurs as small (2-4 mm) clots exhibiting decussate texture.

Chlorite is a secondary mineral replacing biotite. Epidote is also a common secondary mineral, present in small fractures and as an alteration product of hornblende.

Mineral assemblages in the amphibolite include:

- hornblende-plagioclase-biotite-cummingtonite-quartz
- hornblende-plagioclase-garnet-quartz

Migmatitic amphibolite

Black, medium-grained, heterogeneous migmatitic amphibolite is exposed in the N. W. $\frac{1}{4}$ of section 35 (location 14, Plate 1). It is in contact with amphibolite on the southwest slope, and pegmatitic granite on the northeast slope. The contact with amphibolite is gradational whereas the exact granite contact is covered by large boulders.

White, coarse-grained tonalitic stringers, or veins, roughly parallel the regional foliation. Ptygmatic folds are highly contorted and isoclinally folded with morthwest trending fold axes (figure 18). Contacts between granular tonalitic stringers and amphibolitic matrix are sharp and distinct.

A gneissic texture is defined by flattened segregations of granular quartz-plagioclase and irregular streaks of biotite-hornblende (figure 19). Garnet poikiloblasts occur randomly throughout the rock. This unit consists of hornblende (2-4 mm, 22-49 %), plagioclase (1-2 mm, 20-27 %, $An_{55}$), quartz (1-2 mm, 21-30 %), biotite (1-2 mm, 2-18 %), garnet (1-5 mm, 1-7 %) and accessory magnetite, apatite, epidote and zircon.

Figure 18: Outcrop of migmatitic amphibolite with highly contorted ptygmatic folds. Location 14.

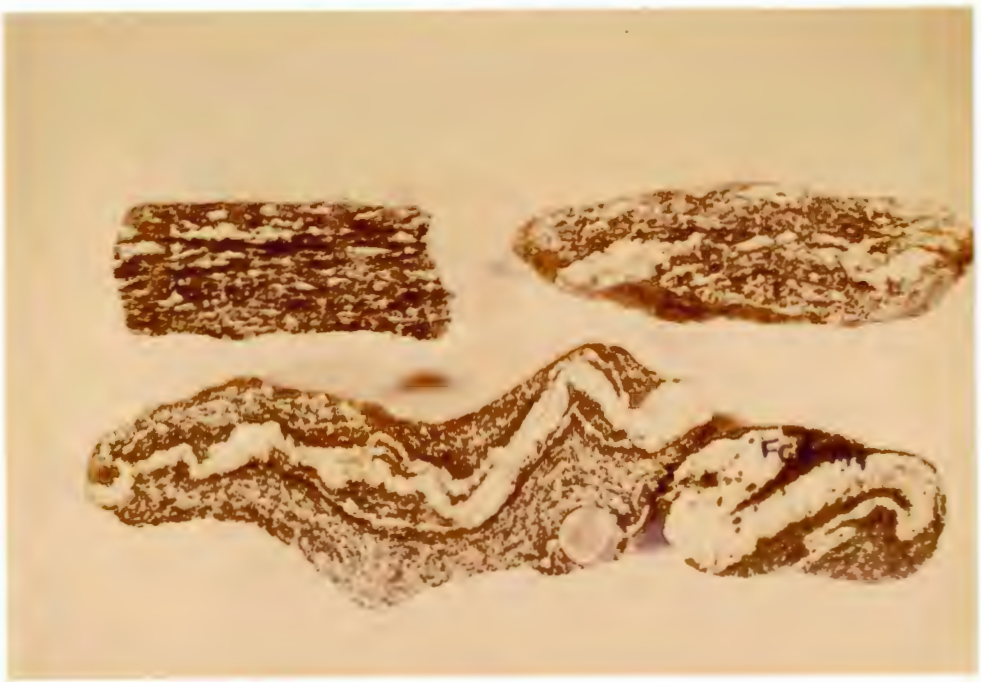

Figure 19: Migmatitic amphibolite.
Upper samples of paleosome.
Lower samples of contorted ptygmatic folds in leucosome of tonalitic composition. Note biotite selvage adjacent to leucosome in lower left sample.
Location 14.

Plagioclase is hypidiomorphic, inequigranular and poikiloblastic with inclusions of biotite, hornblende, magnetite and quartz. Quartz is inequigranular, somewhat elongated and has rounded grain boundaries. Biotite is grown parallel to rational boundaries of hornblende. Hornblende and biotite occur in decussate-granoblastic clots.

Included within this unit is a gneiss deficient in hornblende that is texturally similar to the migmatitic amphibolite. It is not mappable by itself and occurs over a small area (1 x 3 meters wide) on the northeast slope. Coarse, quartz-plagioclase segregations separate wavy biotite streaks (figure 19). It consists of plagioclase (1-6 mm, 19 %, $An_{40}$), biotite (1-2 mm, 37 %), quartz (1-6 mm, 22 %), garnet (1-4 mm, 2 %) and accessory zircon, magnetite and sphene. No hornblende is present.

The leucosome is tonalitic and consists of stringers or veins of medium-to-coarse grained, granular quartz and plagioclase (figure 19). Both quartz and plagioclase are xenomorphic and inequigranular. Quartz exhibits irregular, sutured grain boundaries and is interstitial to plagioclase. Plagioclase ($An_{47}$) is poikiloblastic, partially saussuritized with tear-drop inclusions of quartz.

A selvage of coarse-grained biotite and hornblende is present at the edge of several leucosomes (figure 20). Biotite decreases in size and abundance away from this

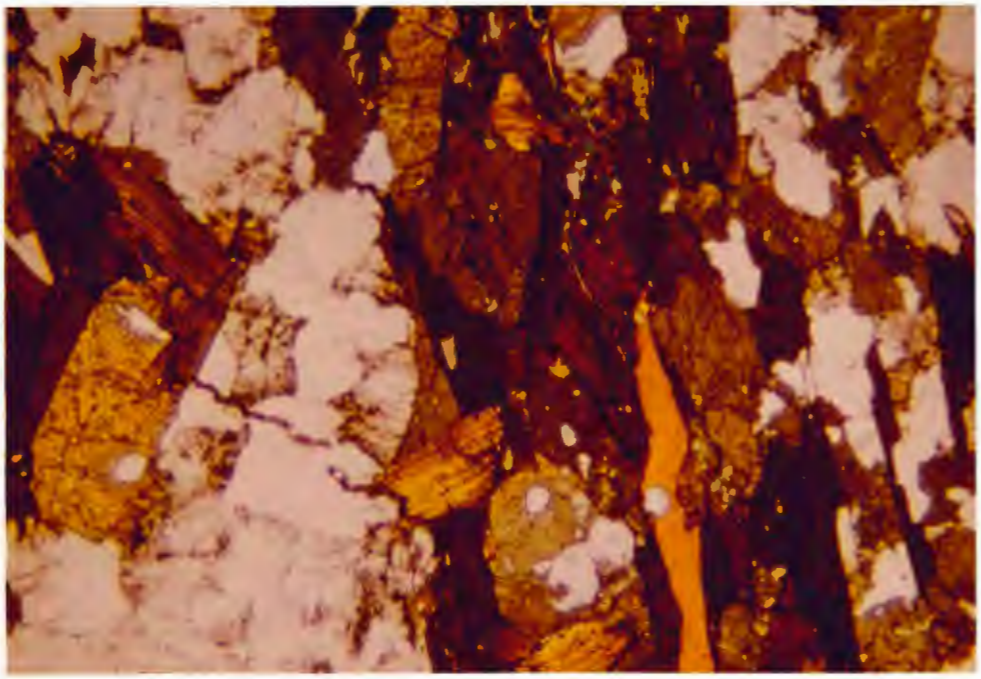

Figure 20: Biotite-hornblende selvage adjacent to leucosome in migmatitic amphibolite. Location 14. FCB 14b.

selvage zone. Convex forms of the leucosomatic quartz-plagioclase segregations against the selvages of biotite and hornblende are common.

Mineral assemblages in the migmatitic amphibolite include:

- hornblende-garnet-plagioclase
- hornblende-garnet-biotite
- hornblende-biotite-plagioclase
- hornblende-cummingtonite-biotite
- garnet-biotite-plagioclase

Garnet augen amphibolite gneiss

Garnet augen amphibolitic gneiss is exposed at location 49, center of section 12, approximately ½ mile directly south of the overlook on the section line of sections 1 and 12, as a dike-like body within granite (plate 1). Reddish porphyroblasts of garnet (1-2 cm), surrounded by light gray medium-grained plagioclase-rich pressure shadows, are contained in a black medium-grained amphibolitic matrix (figure 21).

The garnet augen amphibolite gneiss consists of hornblende (2-3 mm, 44 %), garnet poikiloblasts (0.5-2 cm, 19 %), plagioclase (1-2 mm, 12 %), quartz (1-2 mm, 22 %), minor biotite, opaques and accessory apatite and zircon. The matrix is quite similar texturally and mineralogically to the amphibolite previously described. The lensoid zone surrounding the garnet poikiloblasts consists of plagioclase which is highly altered to sericite and epidote (35-45 %),

slightly strained quartz (30-45 %), and ilmenite (5 %). Hornblende is rarely seen in the lensoid zone.

The poikiloblastic garnet exhibits two stages of growth, identified by a high concentration of inclusions forming an internal grain boundary within the porphyroblast (figure 22). The core is defined by euhedral grain boundaries and contains inclusions of quartz, altered plagioclase, ilmenite and biotite. The overgrowth differs in the following ways: 1) inclusions are less regularly spaced than in the core, 2) there is a greater percentage of inclusions than in the core, and 3) hornblende inclusions are present.

This would suggest that the garnet core is pretectonic. Garnet then nucleated syntectonically about the previously formed garnet core. Foliation defined by prismatic hornblende wraps around the garnet poikiloblast. Some hornblende has also been incorporated into the overgrowth as inclusions.

Mineral assemblages in the garnet augen amphibolitic gneiss include:

- hornblende-plagioclase-quartz
- hornblende-plagioclase-garnet-quartz
- garnet-plagioclase-quartz

Figure 21: Garnet augen amphibolitic gneiss. Garnet porphyroblasts surrounded by light gray, plagioclase-rich pressure shadows contained in a black, amphibolitic matrix. Note overgrowths in garnet in polished sample. Location 49.

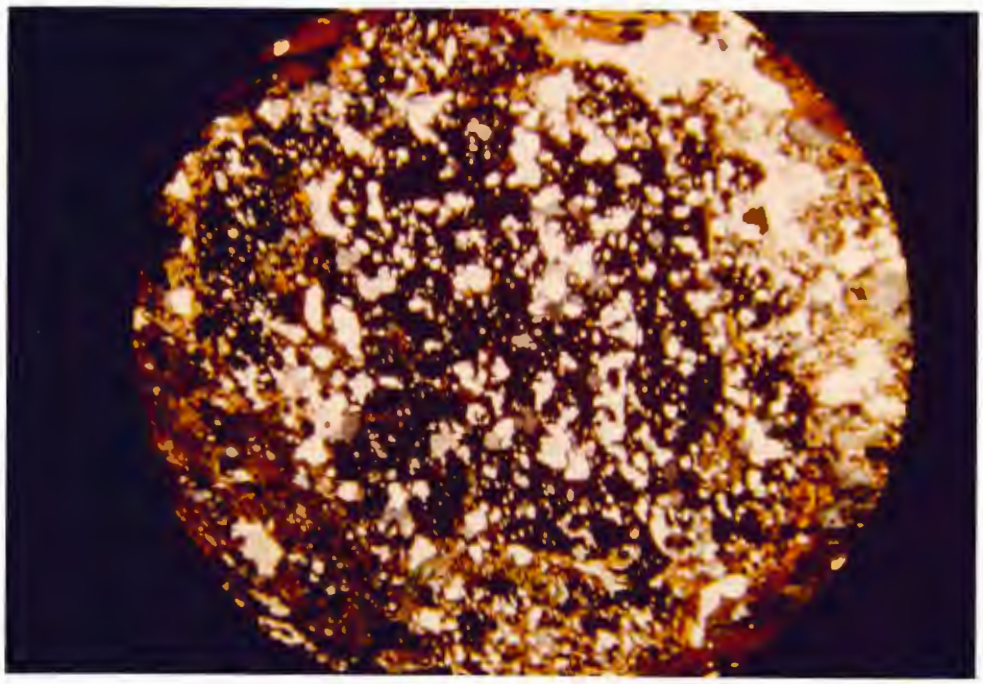

Figure 22: Poikiloblastic garnet with overgrowth. Core contains no hornblende, however, the rim does contain inclusions of hornblende.
Field of view: 13 mm. X-nicols. FCB 49.

## Other gneissic rocks

### Granitic gneiss

Granitic gneiss is exposed along Skyline Drive in the S. E. ¼ of section 2. It is pink, white and gray, medium-grained, foliated and porphyroblastic. Deep red, garnet porphyroblasts (2-4 mm) and magnetite grains (average size 1-2 mm, range up to 2 cm) occur throughout the unit. Texturally these rocks are massive or banded and are cut by leucocratic stringers (2-4 cm wide). These stringers are subparallel to the foliation and are nearly parallel to axial planes of minor isoclinal folds (figure 23).

Massive granitic gneiss is composed of an equigranular (3-5 mm), medium-grained, xenomorphic, interlocking mosaic of microcline-perthite 35-40 %), plagioclase (30 %, $An_{30}$), quartz 25-30 %), magnetite (1 %), and biotite. Plagioclase is saussuritized and has thin, unaltered overgrowth. These overgrowths or rims are only present where plagioclase is in contact with or enclosed by microcline, where vermicular myrmekite is also present. Magnetite commonly occurs as small equant grains (1-4 mm) but elongate grains (1-2 cm long) with secondary biotite overgrowths are also present. Biotite is oriented with its basal cleavage perpendicular to the magnetite grain boundary.

Figure 23: Isoclinal fold in pink, banded granitic gneiss with leucocratic stringer subparallel to axial plane. Location 52.

Banded granitic gneiss consists of alternating dark, fine-grained, biotite-rich bands (2-7 mm wide). The biotite-rich bands consist of fine-grained (1-2 mm), equigranular, xenomorphic interlocking biotite, plagioclase ($An_{30}$), potassium feldspar, garnet, accessory zircon, secondary epidote and sphene. Biotite is replaced by dark green chlorite and sphene. Garnet is in various stages of being replaced by green chlorite, sericite and magnetite-ilmenite.

Pink, medium-grained feldspar-rich bands are generally similar in composition and texture to the massive variety of granitic gneiss described above. However, very coarse-grained bands are present. In these, plagioclase (3 mm-2 cm) is xenomorphic, contains very fine patches of microcline (antiperthite) and has thin, unaltered overgrowths. Microcline (4-8 mm) is likewise xenomorphic. Quartz (2-6 mm) is xenomorphic and interstitial to the plagioclase and potassium feldspar. Concentrations of garnet (1-2 mm) and biotite are commonly found along the edges of these pink, coarse-grained bands, and therefore define a plane of foliation.

Leucocratic stringers are light gray, fine-to-medium grained tonalite. They consist of granoblastic, equigranular (1-3 mm) plagioclase ($An_{38}$, 55 %), interstial quartz (45 %) and minor garnet.

Hornblende-cummingtonite-garnet gneiss

Rusty brown, weathered, blocky chunks of hornblende-cummingtonite-garnet gneiss are exposed at the center of S. ½ of section 35. Texturally and mineralogically, it varies from a medium-grained (2-5 mm) quartz-garnet granofels to a layered hornblende-cummingtonite-quartz-garnet gneiss (figure 24).

The granofels consists of euhedral, poikiloblastic garnet (55 %, 2-5 mm), quartz (20-25 %, 1-2 mm), magnetite (13 %, 1 mm), plagioclase (9 %, 1-2 mm), minor hornblende and biotite, secondary chlorite, and accessory apatite and zircon. Hornblende-cummingtonite-quartz-garnet gneiss consists of euhedral, poikiloblastic garnet (36 %, 2-4 mm), green prismatic hornblende (22 %, 1-2 mm), cummingtonite (4-5 %, 1-2 mm), quartz (10-15 %, 1-2 mm), plagioclase (10 %, 1-2 mm), magnetite (5 %), minor apatite, secondary chlorite and epidote, and accessory zircon. Plagioclase has been saussuritized in both the granofels and gneiss.

The subhedral to euhedral garnet typically shows three habits: 1) poikiloblastic with subrounded inclusions of quartz, opaques, minor biotite and plagioclase, 2) cores relatively free of inclusions with rims rich in inclusions of plagioclase, quartz and amphibole which parallel garnet grain boundaries with a surrounding rim of garnet, and 3) atoll garnet (figure 25).

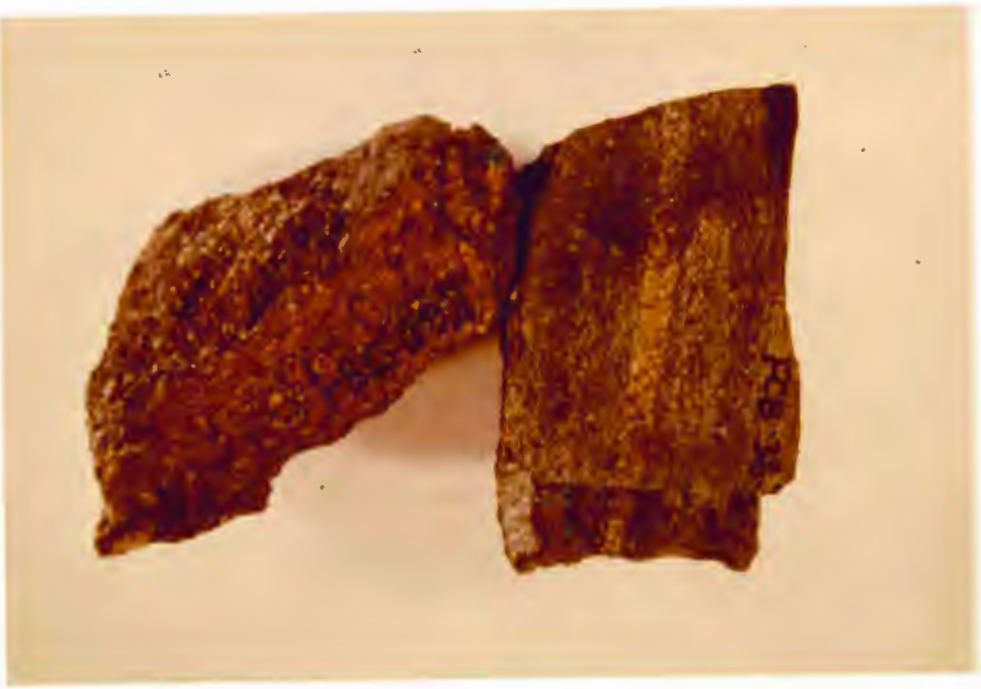

Figure 24: Left, sample of hornblende-cummingtonite-quartz-garnet gneiss. Right, sample of quartz-garnet granofels. Location 38.

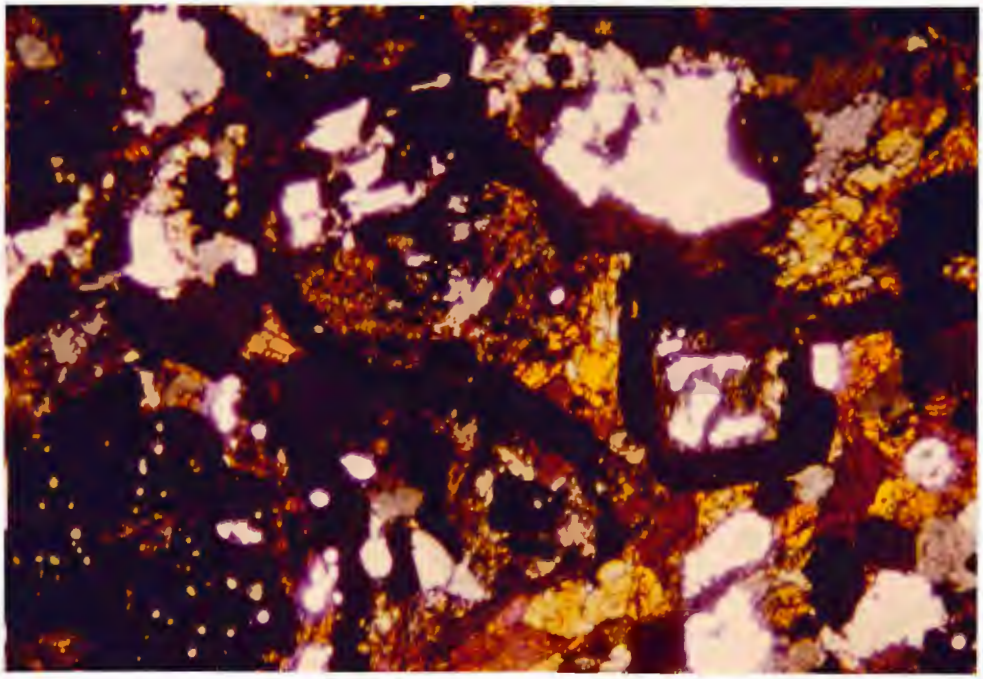

Figure 25: Three habits of garnet in quartz-garnet granofels. Lower left: Poikiloblastic. Bottom center: Core of garnet with rim of plagioclase, quartz and amphibole with a surrounding rim of garnet. Right center: Atoll garnet. Field of view: 6 mm. X nicols. FCB 38-3.

Amphibole defines a foliation in which laminae of hornblende (1-3 mm) alternate with laminae (1 mm) of hornblende-cummingtonite. Hornblende and cummingtonite both exhibit decussate-granoblastic texture. Hornblende is distinguished from cummingtonite by its 2V, pleochroic formula and twinning.

Mineral assemblages in the hornblende-cummingtonite-garnet gneiss include:

- garnet-hornblende-cummingtonite-quartz
- garnet-hornblende-plagioclase-quartz
- garnet-plagioclase-quartz
- hornblende-cummingtonite-quartz
- hornblende-plagioclase-quartz

Garnet-cordierite-anthophyllite gneiss

Light gray, medium-to-coarse grained, poikiloblastic, foliated garnet-cordierite-anthophyllite gneiss is exposed on the southwest slope of Bountiful Ridge in the N. W. $\frac{1}{4}$ of section 35 (location 31, Plate 1). It occurs as a small lobe adjacent to amphibolite and garnet-cordierite-biotite gneiss. It is found mainly as float, in boulders 1-3 meters across, which have slumped down slope from the top of the ridge.

Garnet-cordierite-anthophyllite gneiss consists of plagioclase (1 mm, 30-35 %, $An_{56}$), quartz (1 mm, 20-25 %), pink, poikiloblastic garnet (1-12 mm, 3-9 %), prismatic

anthophyllite (2-15 mm, 20-27 %), pale-blue cordierite (1-3 mm, 13 %), brown platy biotite (1-2 mm, 2 %) with some opaques and accessory apatite, epidote and zircon. Rare cummingtonite and actinolite are also present.

Foliation is defined by irregular, wavy bands (several grains thick) of cordierite + anthophyllite + garnet + biotite in an inequigranular, interlocking mosaic of quartz and plagioclase (figure 26).

Hypidiomorphic garnet is poikiloblastic with inclusions of quartz, opaques, plagioclase and cordierite. It is rimmed by cordierite and plagioclase, and is wrapped by foliated anthophyllite (fingre 27). Garnet occurs in two grain sizes: 1) typically 1-4 mm at location 31, and 2) coarser, up to 12 mm at location 42 (Plate 1).

Cordierite surrounds the garnet poikiloblasts (figure 27) and occurs as a symplectic intergrowth with quartz (figure 28). Cordierite is identified by its characteristic yellow-green pinite and net-textured alteration (figures 28 and 29). Yellow pleochroic haloes around included zircons also aids identification (figure 29). Biotite shows no preferred orientation but often exhibits rational grain boundaries with anthophyllite. Accessory minerals include opaques, apatite, epidote and zircon

Fine-grained garnet-cordierite-anthophyllite gneiss exists one half mile southeast, at the center of the S. $\frac{1}{2}$ of section 35 (location 42, Plate 1). Similar mineralogy

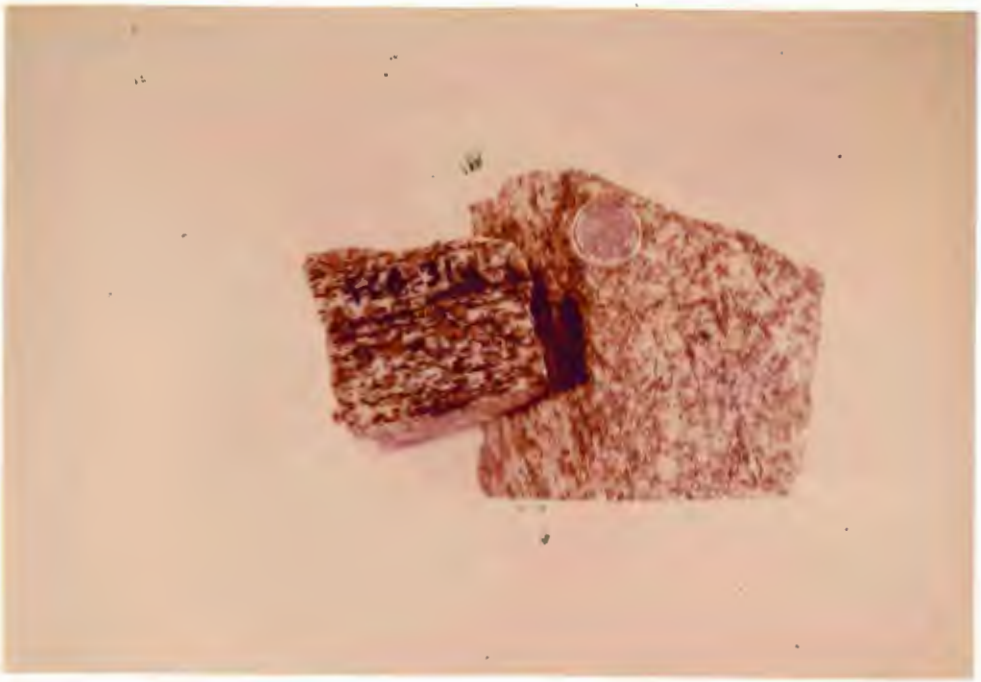

Figure 26: Hand sample of cordierite-garnet-anthophyllite gneiss. Well defined foliation formed by prisms of anthophyllite with red garnet porphyroblasts disseminated through rock. Location 31.

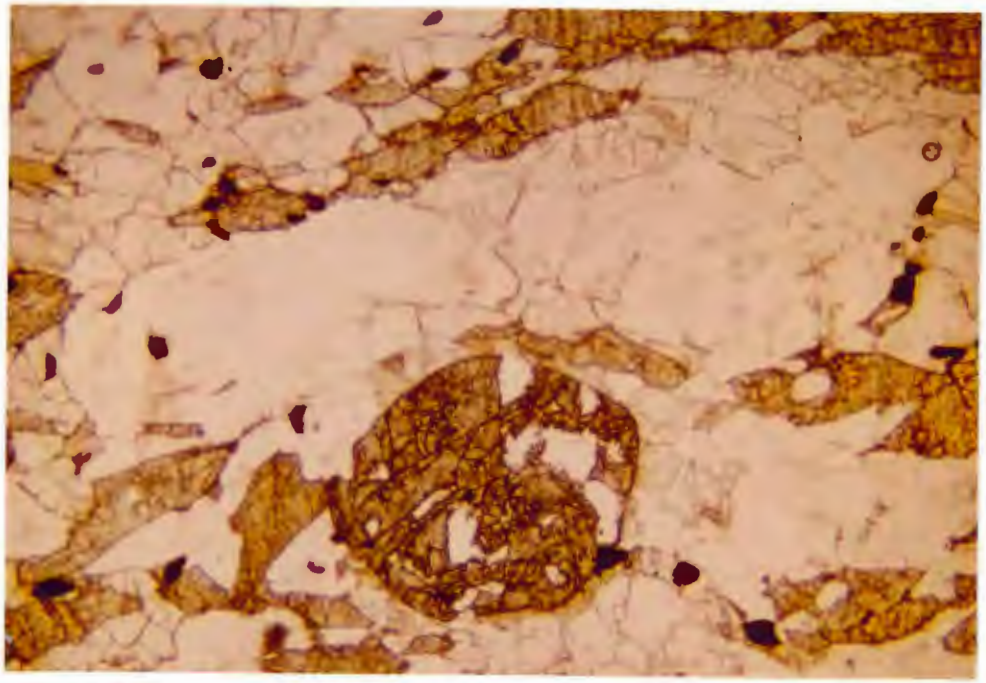

Figure 27: Textural relationship of garnet-cordierite anthophyllite gneiss. Anthophyllite wraps around cordierite and garnet, cordierite encloses garnet. Cordierite has slightly higher relief than quartz and plagioclase due to pinite alteration. Field of view: 6 mm. Plain light. FCB 31a.

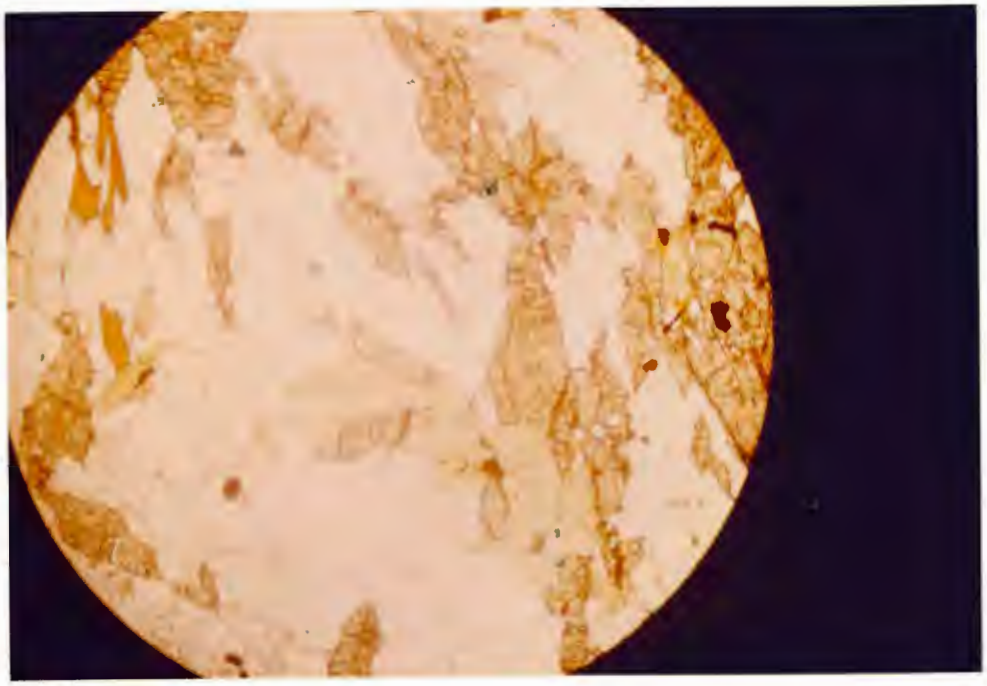

Figure 28: Characteristic yellow-green pinite alteration of cordierite. Note the symplectic intergrowth of cordierite with quartz.
Field of view: 5 mm. Plain light. FCB 31a.

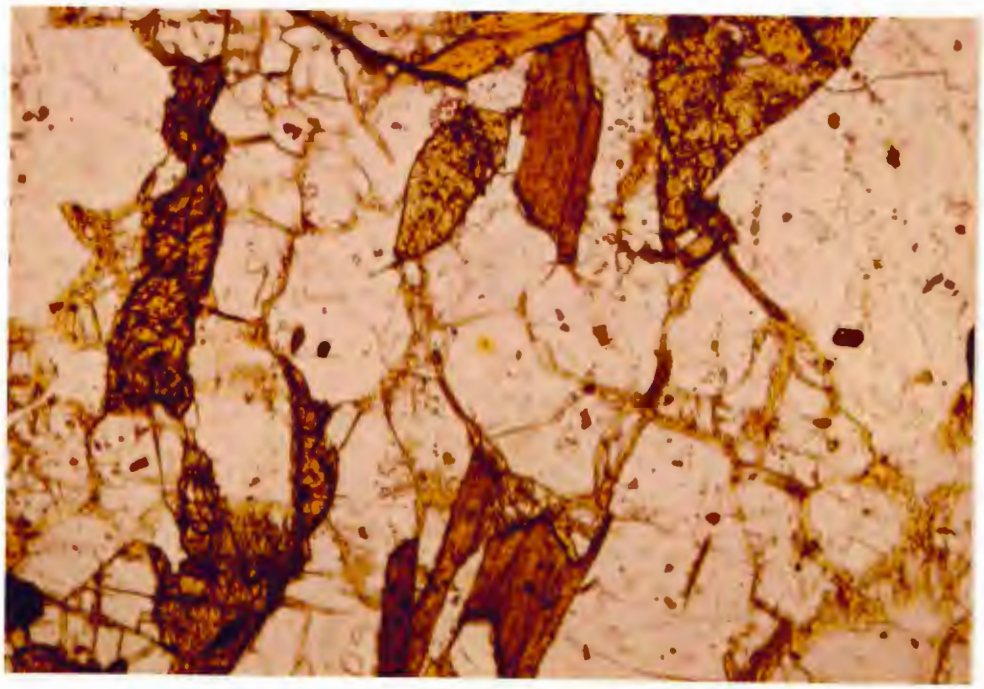

Figure 29: Yellow pleochroic halo (center) about included zircon within cordierite. Net-textured alteration of cordierite. Anthophyllite, biotite, and cordierite.
Field of view: 6 mm. Plain light. FCB 31a.

and textures to that discussed above are present. However, some major differences occur in a zone adjacent to the pegmatitic granite, where large gray poikiloblastic clots, up to 2 cm, in size, of cordierite define a plane of foliation. Elongate amphibole defines a northwest trending mineral lineation.

In thin section, these clots are now composed of epidote-chlorite and coexisting cummingtonite-anthophyllite-actinolite with minor sericite and remnant plagioclase Cummingtonite rims the clots and is generally coarser grained than the amphibole within the clots (anthophyllite-actinolite).

One section showed very large blades of poikiloblastic anthophyllite (up to 3 cm) with elongate plagioclase inclusions parallel to the anthophyllite cleavage. Also, fine-grained (1-4 mm) cummingtonite cross-cuts anthophyllite.

Pertinent mineral assemblages include:

- cordierite-plagioclase-anthophyllite
- cordierite-plagioclase-biotite
- cordierite-plagioclase-garnet
- cordierite-garnet-anthophyllite
- cordierite-garnet-biotite
- cordierite-biotite-anthophyllite
- garnet-anthophyllite-biotite
- garnet-anthophyllite-plagioclase
- garnet-biotite-plagioclase
- plagioclase-anthophyllite-biotite

plus quartz.

## Granites

### Pegmatitic granite

Granitic rocks vary texturally and compositionally from pegmatitic-graphic granite to inequigranular, coarse-grained granite-granodiorite. They vary in color from pink to light gray or white. Color and/or texture change over distances of several feet.

Contacts with country rocks are commonly obscured by plant growth. Sharp, concordant contacts are observed on top of Bountiful Peak where granitic dikes intrude laminated biotite-quartz-feldspar gneiss (location 28, Plate 1). Gradational contacts, over two to three feet, are common at contacts with migmatitic zones (location 14, Plate 1).

The granite as a whole consists of approximately 40-50 % K feldspar, 25-30 % plagioclase, 20-30 % quartz and minor amounts of muscovite, biotite, sillimanite and garnet. The pink granite is typically pegmatitic, with graphic intergrowths of microcline-perthite and quartz up to 1.3 meters long (4 feet). Inequigranular, coarse-grained textures are less common. Plagioclase ($An_{12}$) occurs as very fine blebs along grain boundaries of microcline in graphic intergrowths (figure 30).

The gray granite is typically inequigranular (3 mm to pegmatitic (10 cm) ). Graphic intergrowths are less

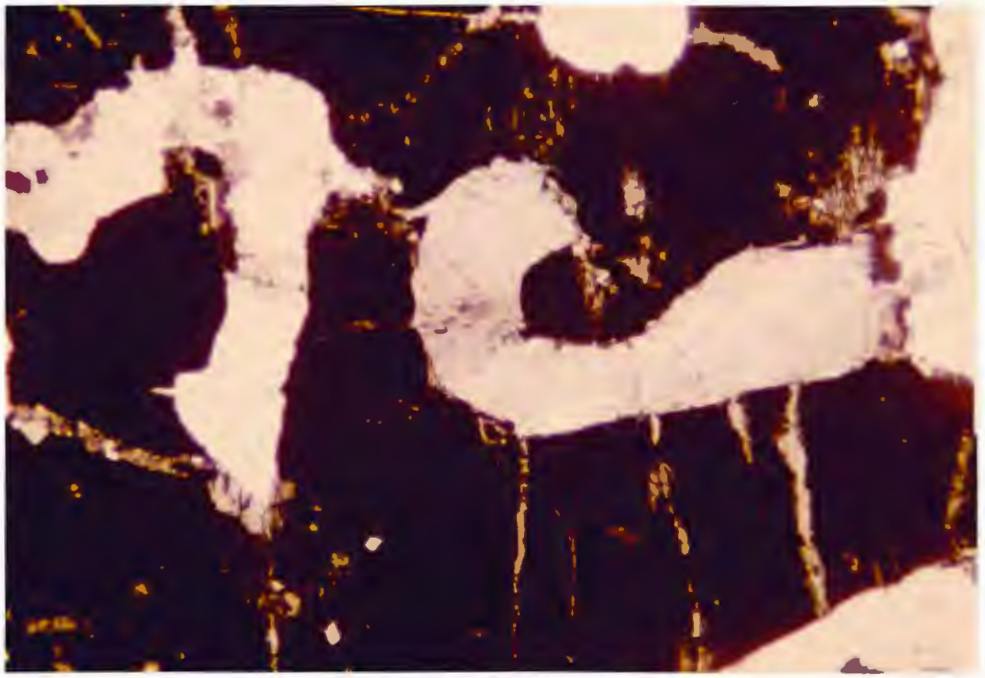

Figure 30: Graphic texture in granite. K feldspar, quartz and minor plagioclase. Field of view: 6 mm. FCB 13.

common than in the pink granite. Coarse-grained xenomorphic microcline-perthite and sericitized plagioclase are bounded by interstitial, medium-grained plagioclase, microcline and quartz. Microcline is typically white, but occurs as deep blue, patchy, hypidiomorphic grains (up to 10 cm) at locations 2 and 59 (Plate 1). Quartz is highly strained and exhibits mortar texture. Myrmekite is common in the interstitial groundmass.

Biotite schlieren are found sporadically within the inequigranular granite and define a foliation which is nearly parallel to the regional foliation.

It is not uncommon to find aluminous minerals present in the granitic rocks. Muscovite, sillimanite and garnet are common constituents of the granite. Muscovite and sillimanite occur as light green, greasy, matted intergrowths. Garnet is xenomorphic to hypidiomorphic (ranging from 0.5 cm to 8 cm). Fresh garnet is pink, whereas garnet that is partially psuedomorphed by biotite is blood red. It also occurs as a radial, graphic intergrowth with quartz (up to 4 cm in diameter -- location 34, Plate 1).

Sheared granite

Shear zones, 10-20 meters wide, on the north slope of Bountiful Peak are recognized as green, mottled, highly altered granite (locations 16 and 17, Plate 1). Grains

are xenomorphic, elongated, and range up to 2 cm in length. Feldspar is completely altered to sericite and chlorite. Quartz exhibits mortar texture and is highly recrystallized (figure 31). Monazite occurs as light brown, euhedral grains (1-6 mm) which may be partly metamict. It is locally confined to zones of shearing.

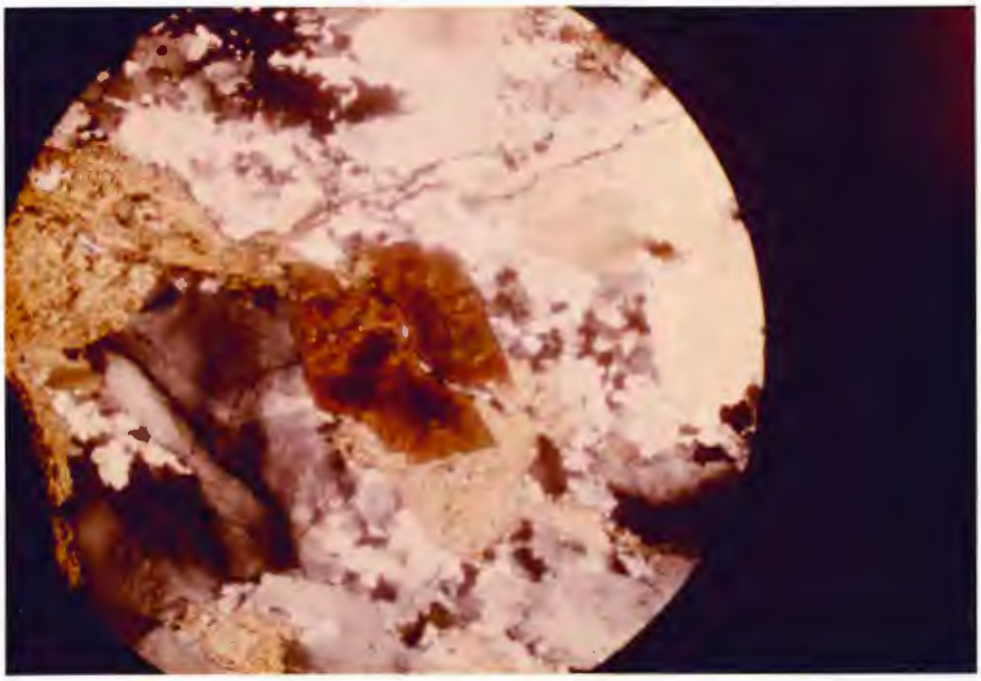

Figure 31: Sheared granite with zoned monazite. Note the high degree of alteration in the feldspar (sericite - chlorite) and the well developed mortar texture in quartz.
Field of view: 6 mm. X-nicols. FCB 16b.

## Structure of the Farmington Canyon Complex

The general structure of the Farmington Canyon Complex previously has been mapped by Eardley and Hatch (1940). They found a large open anticline trending N. 60 W. and plunging 15-20 northwest through Bountiful Peak (Plate 1). However, the structural complexity is readily recognized as one looks at the small scale structural features.

### Folds and Axial Surfaces

Numerous tight and isoclinal folds are present in the highly metamorphosed rocks of the Farmington Complex. This can best be observed in the laminated biotite-quartz-feldspar gneiss (Figure 32) and in the migmatitic gneisses.

Figure 32: Isoclinal folding present in the Farmington Canyon Complex.

Quartz-sillimanite knots, in addition to forming a very distinctive mineral lineation, were found to be nearly axial planar to the folds (Figure 33A & 33B). In some instances, the quartz-sillimanite knots were also found to fan across the fold (Parallel to hammer in figure 33B).

The contour diagram of poles to axial planes (Figure 34A) further illustrates the structural complexity of the Farmington Complex. The scatter makes the interpretation difficult and will be discussed later in more detail. Two main clusters are apparent, possibly indicating two separate periods of deformation. However, both sets of axial planes have northwest trending fold axes which further complicates the interpretation. The general strike of the axial planes is northwesterly but the two sets differ drastically in their dip: 1) N. 40 W., 68 S.W. and 2) N. 64 W., 20 N.E.

Foliation: Compositional Layering and Schistosity

Compositional layering in the Farmington Canyon Complex is best observed in the laminated biotite-quartz-feldspar gneiss in which fine biotite-poor layers of quartz and feldspar (typically 3-10 mm wide) alternate with thin biotite-rich layers (about 1-2 mm wide). This layering, which is really a spaced schistosity, can often be traced for the length of the outcrop, sometimes several tens of meters.

Compositional layering is also present in the amphibolitic units, especially in the quartz amphibolites in which coarse-

Figure 33A

Sample
Locality #21

Figure 33B

Sample
Locality #28

Figure 33A: Axial planar quartz-sillimanite knots parallel to pencil.

Figure 33B: Axial planar quartz-sillimanite knots fanning across an isoclinal fold (parallel to hammer).

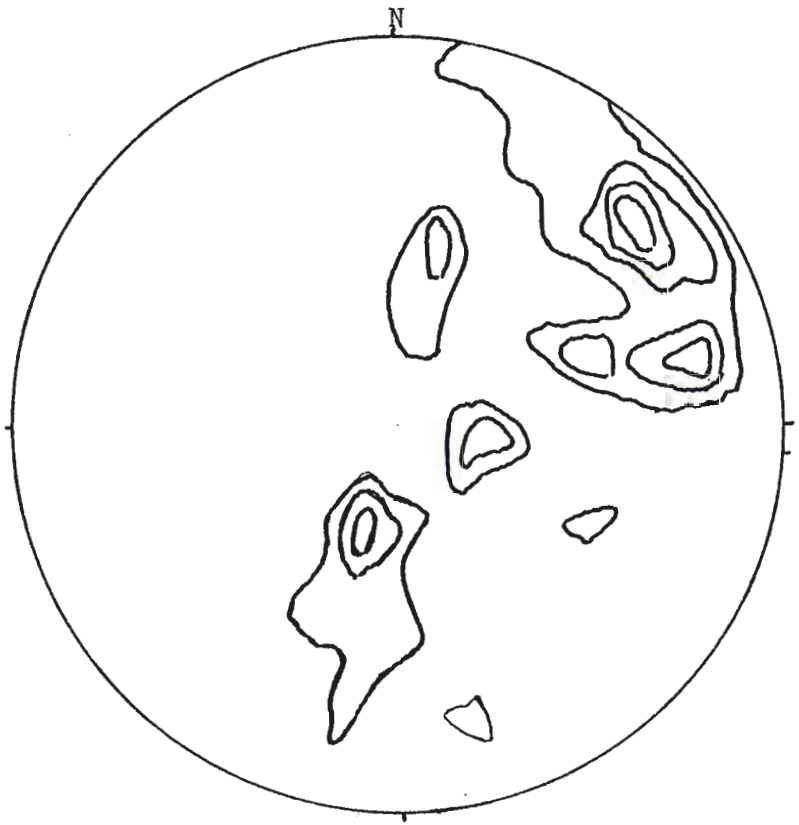


Figure 34A. Poles to axial planes
Two main maxima at:
1) N. 40 W., 68 S.W.
2) N. 64 W., 20 N.E.
3-6-9-12% per 1% area
(36 measurements)

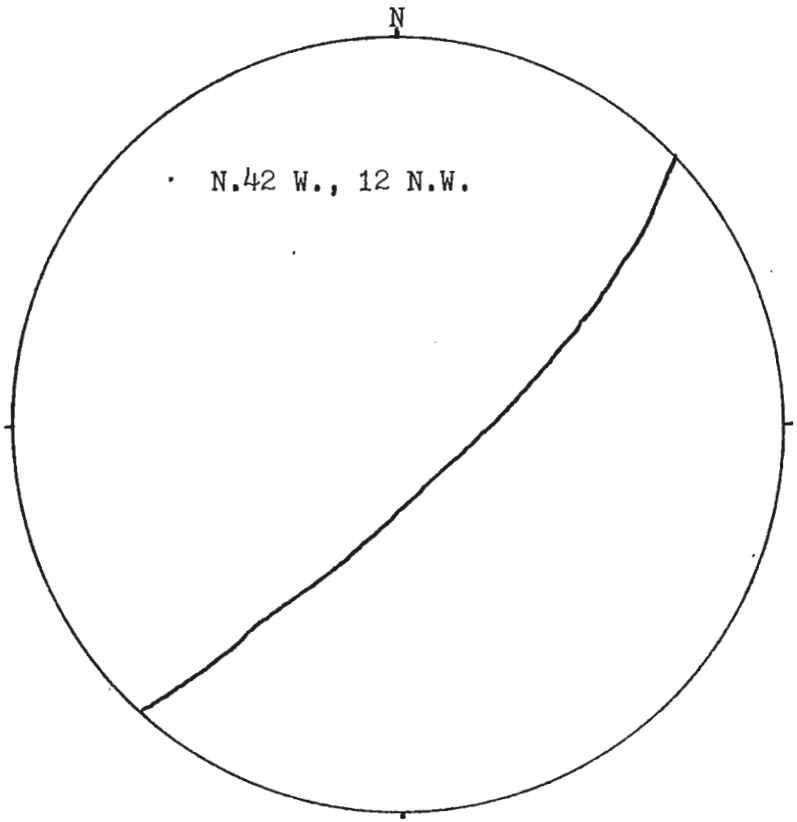


34B. Rough girdle of poles to axial planes representing fanning of axial planes about a fold axis: N. 42 W., 12 N.W.

grained quartz and plagioclase bands (2-8 mm) alternate with biotite-plagioclase-hornblende layers.

The biotite and hornblende also define a schistosity. In some instances, the hornblende is also alligned to define a lineation.

Biotite defines a well developed schistosity in most of the biotite-quartz-feldspar gneisses. The biotite was found to wrap around most minor folds. In cases where the fold was tight or isoclinal, biotite and often sillimanite together defined an axial planar foliation.

From nearly 100 measurements of biotite foliation and compositional layering, the major fold axis was found to trend approximately N. 65 W. and plunge 13-20 northwest (figure 35). This corresponds reasonably well with the work of Eardley and Hatch (1940) who mapped an open anticline trending N. 60 W., plunging 15-20 northwest through Bountiful Peak.

Lineations: Fold Axes

Two maxima can be seen in a stereonet of fold axes, (Figure 36A), perhaps indicating two periods of deformation. The first developed folds with fold axes in a northwesterly direction of N. 51 W., plunging 15 N. W. A minor trend was recognized at only a few outcrops (e.g. Lenticular gneiss, sample location #7) and measured S. 40 W., plunging 40 S.W. A refolded isoclinal fold was also found with both fold axes trending in a similar northwesterly direction.

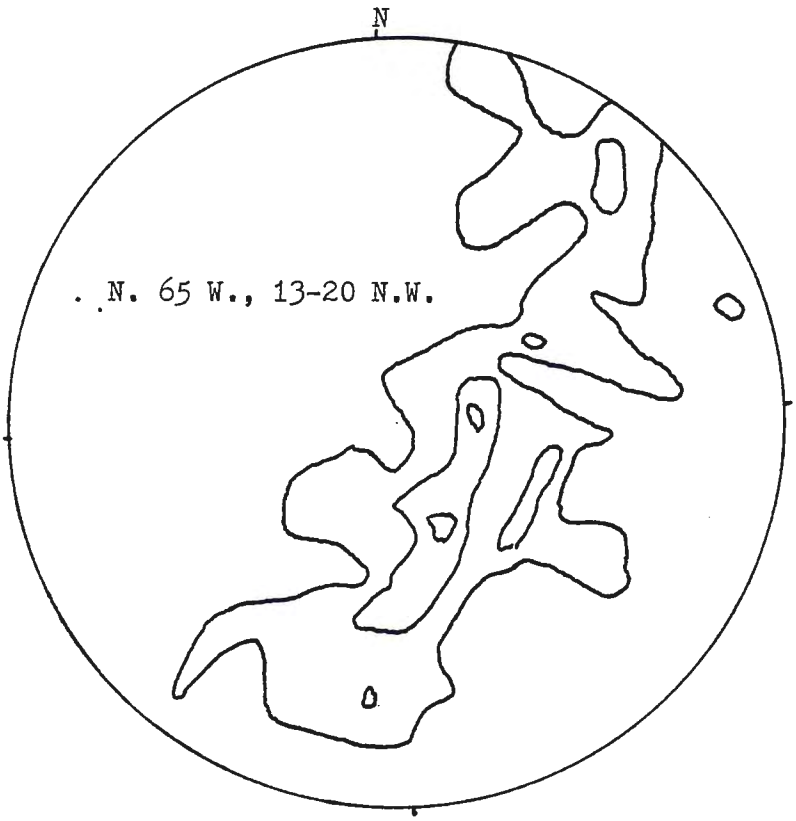


Figure 35: Poles to foliation & compositional layering with major fold axis of approximately N. 65 W., 13-20 N.W. Contour interval of 2-4-6% per 1% area. (94 measurements)

Mineral Lineations

Common mineral lineations include quartz-sillimanite knots, biotite, amphibole and elongate quartz-feldspar lenses. Figure 36B, which includes all mineral lineations, defines a major northwest trend between N. 59 W. - N. 39 W., plunging 17-22 N.W., and a minor southwest trend of S. 60 W., plunging 40 S.W.

Pale white-to-green quartz-sillimanite knots occur as very distinctive lineations in the laminated biotite-quartz-feldspar gneiss. These knots are often as large as 15X2.5 cm and trend N. 60 W., plunging 15-18 N.W. (Figure 36C), nearly parallel to the major trend of the fold axes. This would indicate formation of these knots during the same deformational event that produced the northwest trending fold axes.

Figure 36D shows the lineation of biotite to trend N. 36 W. and plunge 22 N.W. A minor southwesterly trend is observed, S. 60 W. and plunging 40 S.W., that parallels the minor southwesterly trend of the minor fold axes.


Figure 3.6A :

Stereonet showing fold axes with two main maxima:
1) N. 51 W., 15 N.W.
2) S. 40 W., 40 S.W.
Contour interval of 2-4-8-12-16% per 1% area. (62 measurements)

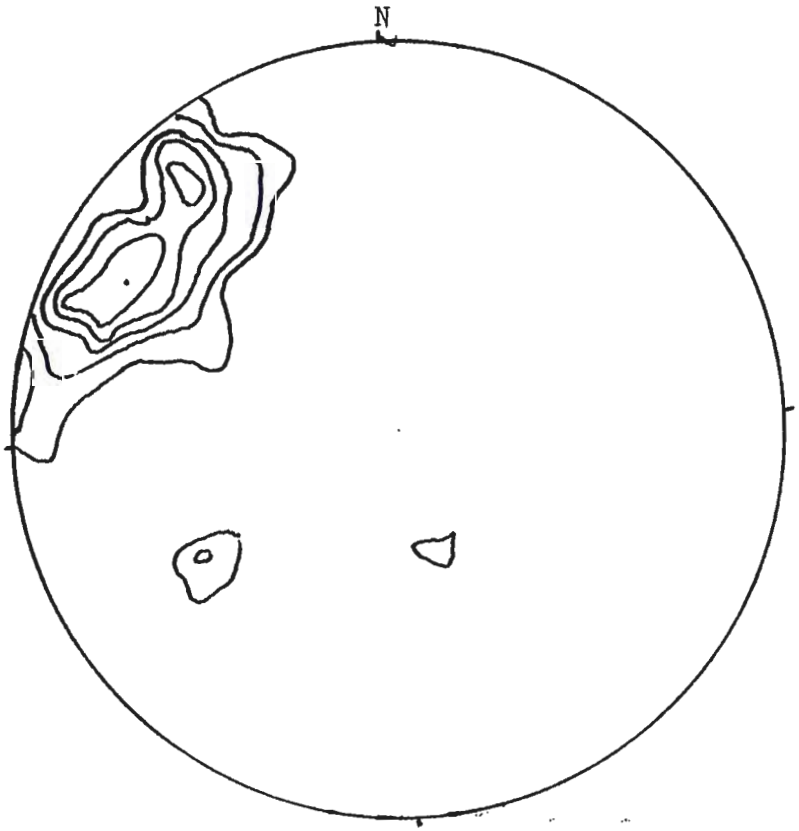


Figure 3.6B :

Stereonet showing all mineral lineations with two dominant northwesterly maxima:
1) N. 59 W., 22 N.W.
2) N. 39 W., 17 N.W.
And one minor maxima: S. 60 W., 40 S.W.
Contour interval of 2-4-8-12-16% per 1% area. (50 measurements)

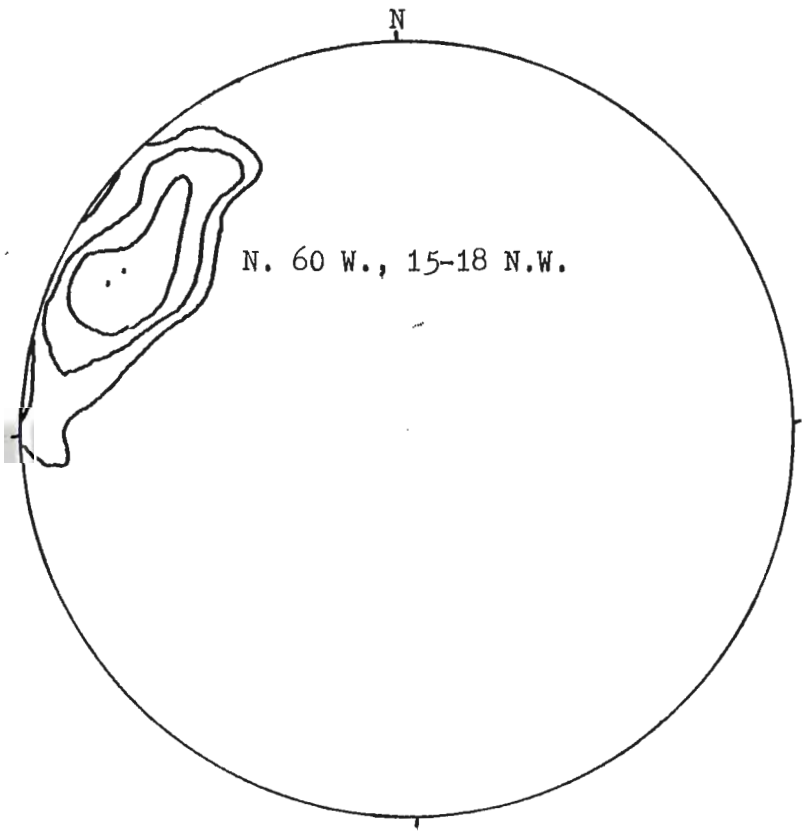


Figure 36C:

Stereonet showing lineation of quartz-sillimanite knots: N. 60 W., 15-18 N.W. Contour interval of 4-8-16% per 1% area. (25 measurements)

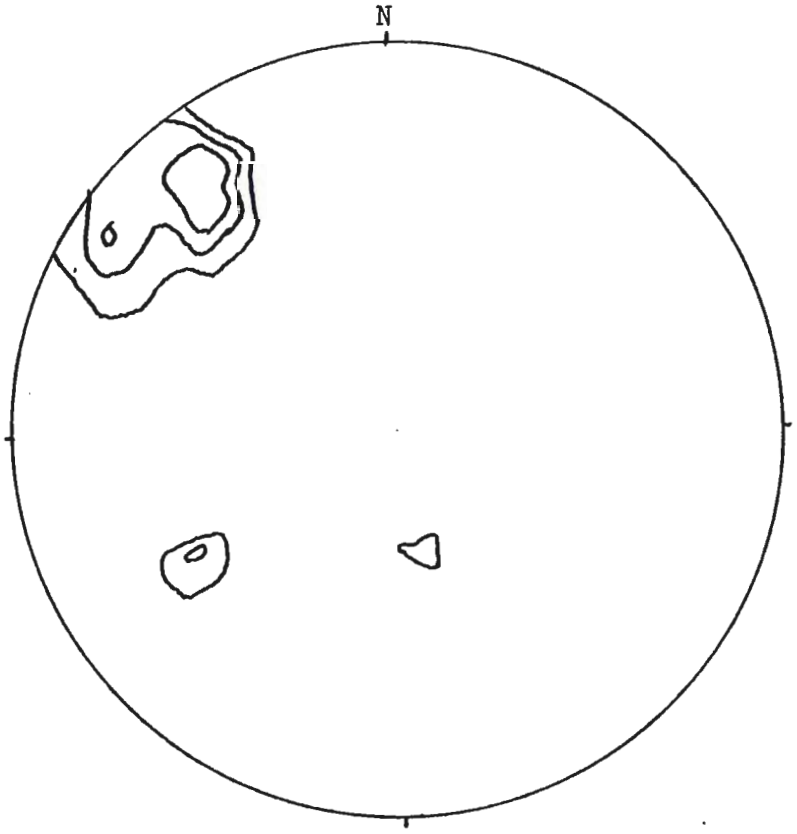


Figure 36D:

Stereonet showing lineation of biotite
Dominant trend: N. 36 W., 22 N.W.
Minor trend: S. 60 W., 40 S.W.
Contour interval of 6-12-18% per 1% area. (17 measurements)

Interference Patterns Produced by Two Successive Foldings

Superposition of two sets of folds results in a particular interference pattern determined by the orientation relationships of the component fold systems (Ramsey, 1967). This may be likened to the pattern of interference caused by the intersection of two sets of waves. Figure 37 describes the relationship between two wave forms in a superimposed fold system.

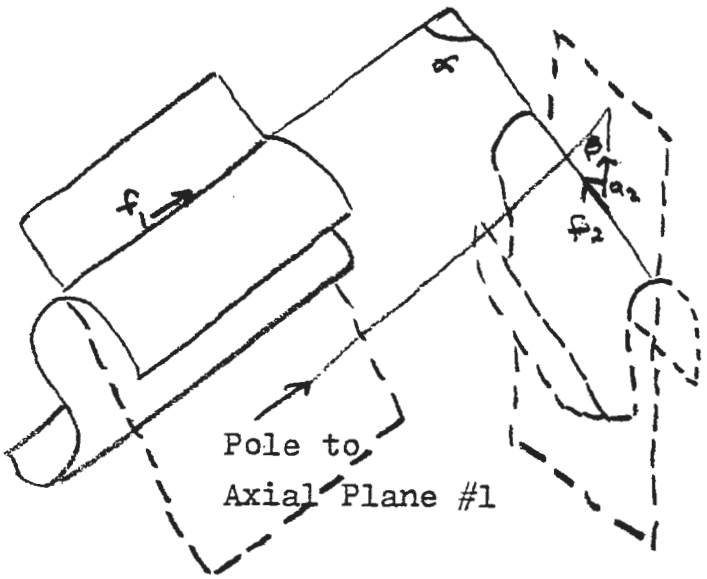


Figure 37
Superposition of two folds (after Figure 10-2 of Ramsey, 1967, Page 521)

$f_1$, $f_2$: fold axes
$a_2$: flow direction of the superimposed movement.

Three basic types of patterns occur depending on the variance of angles $\alpha$ and $\beta$ as shown in Figure 38.

In the present study, the type 1 interference pattern has been recognized, but is rare. Crossing antiforms and synforms result in the formation of domes and basins, respectively (Figure 39).

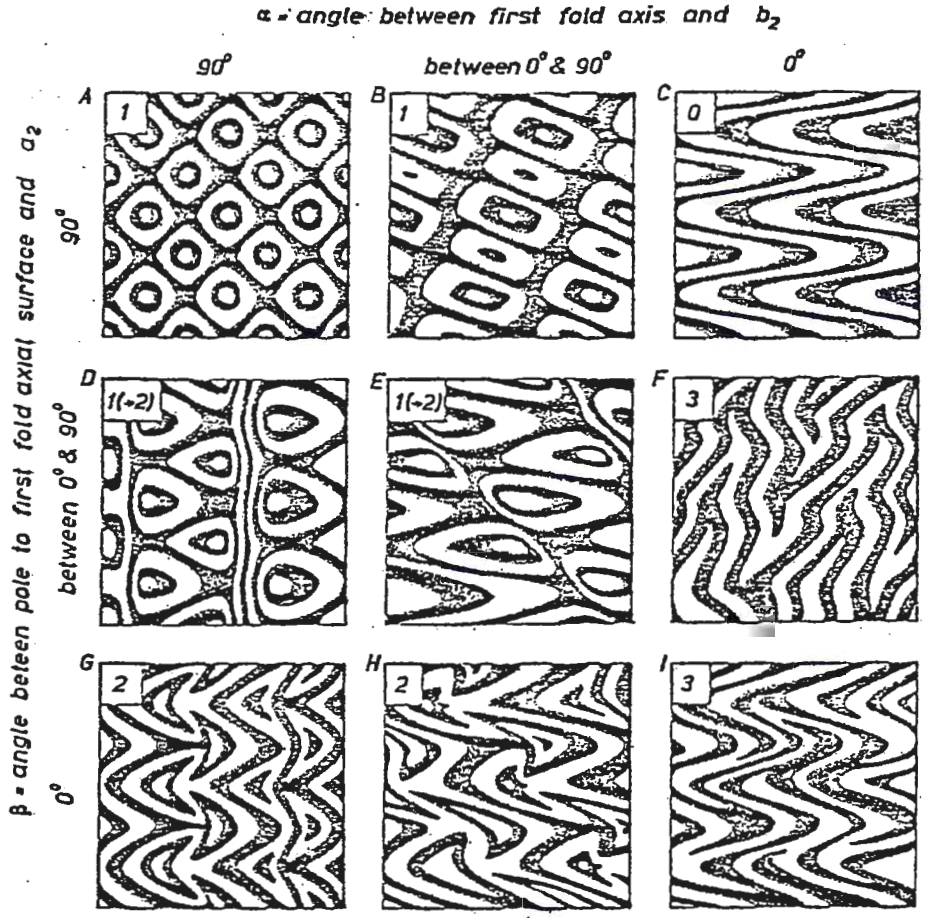


**Figure 10-13**

*Various types of two-dimensional interference patterns and their dependence on the angles α and β (Fig. 10-2). Where α = 0 and β = 90° (C), the two sets of folds have parallel axial surfaces and axes, and there is no characteristic pattern of interference. All other variations of α and β produce patterns of types 1, 2, or 3, or transitional forms (D and E).*

Figure 38 (Figure 10-13 of Ramsey, 1967, page 531)

Also, the type 3 interference pattern has been observed, but is difficult to find (Figure 40). Coaxial folding results from the superposition of two groups of folds so that the two axis orientations are nearly parallel and the two axial surface orientations are non-parallel.

If tight and isoclinal first folds of this structural interference pattern (type 3) formed, it may be difficult to detect the hinge zones of the first folds. Figure 40.

Figure 39: Type 1 interference pattern -- dome and basin fold (Sample location 28).

below shows this structural pattern is present. Undetected hinge zones may account for the thick sequence of fine, continuous layering in the laminated biotite-quartz-feldspar gneiss. Therefore, the quartzo-feldspathic layers may represent repeated layering and not a true stratigraphic thickness.

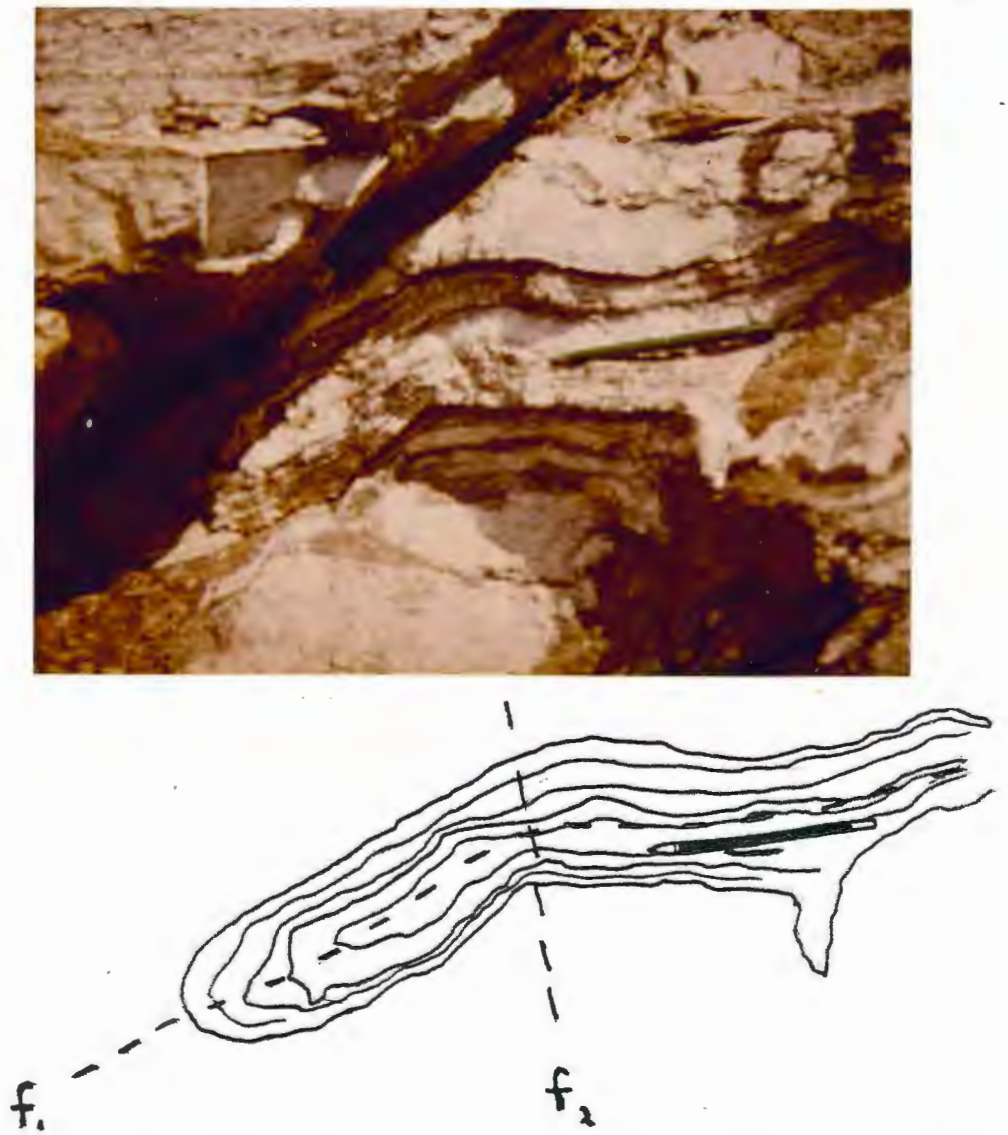


Figure 40: Type 3 interference pattern -- refolded isoclinal fold (Sample location 45).

## Shear Zones

Two prominent shear zones occur on the north slope of Bountiful Peak in the N.W. ¼ of section 27. One zone also occurs in the S.W. ¼ of section 26. These zones are 40 to 60 feet wide, trending approximately east-west and have a mottled light green coloration. The shear zones are found in granite or along the contact between granite and laminated biotite-quartz-feldspar gneiss. Pale-green, altered laminated biotite-quartz-feldspar gneiss is associated with the shear zones. Microscopically, quartz exhibits mortar texture and has undergone slight to moderate recrystallization. Feldspar has been highly altered, mainly to sericite, but some chlorite is also present.

## Relationship of Granite to Country Rocks

Coarse-grained, pegmatitic granite is exposed along the crest of Bountiful Ridge. Both concordant and discordant contacts are observed (Figure 41A & Figure 41B). Biotite schlieren (Figure 42) can be observed sporadically within the granite but perhaps can be best observed along the Morgan-Davis County line in the northern half of section 2, R.1 E., T.2 N. Here, the schlieren appear to have undergone very little rotation and can be observed to be nearly parallel to the compositional layering in the nearby laminated biotite-quartz-feldspar gneiss.

Figure 41A
Concordant contact of granite parallel to biotite foliation in laminated biotite-quartz-feldspar gneiss.

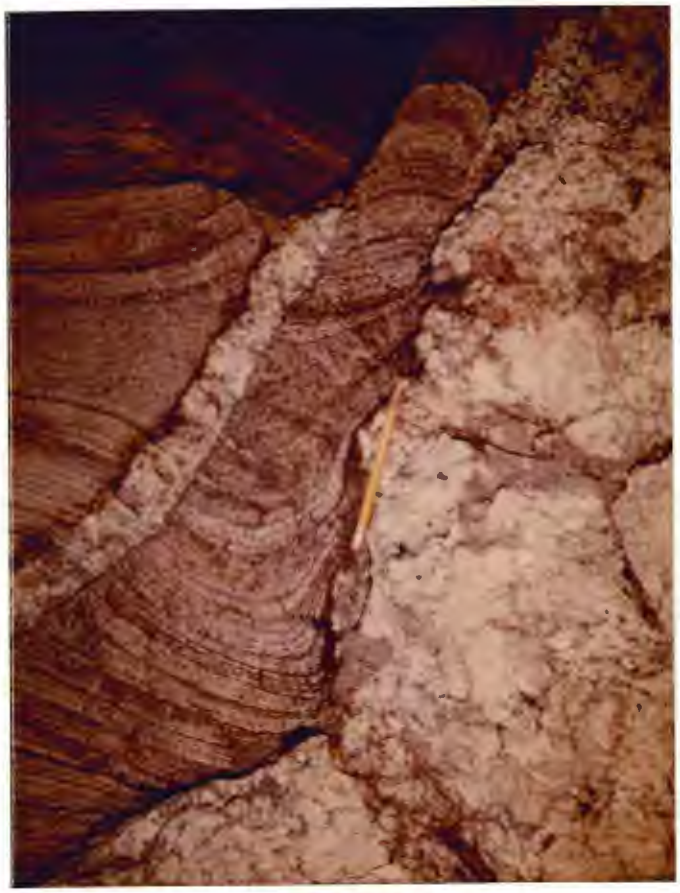

Figure 41B
Discordant contact of Granite in laminated biotite-quartz-feldspar gneiss.

Figure 42: Biotite schlieren within the granite (Sample location 58).

Important outcrops: Lenticular Gneiss (Sample location #7)

The lenticular gneiss is characterized by elongate quartz-feldspar lenses that form a northwest trending lineation. These elongate lenses were deformed during the same deformational event that formed the northwest trending fold axis and quartz-sillimanite knots as they are lineated parallel to the fold axes. Figure 43 shows evidence for a second deformational event as these elongate lenses have themselves been folded. The pencil lies in the trace of the axial surface. The fold axis trends S. 46 W. and plunges 41 S.W.

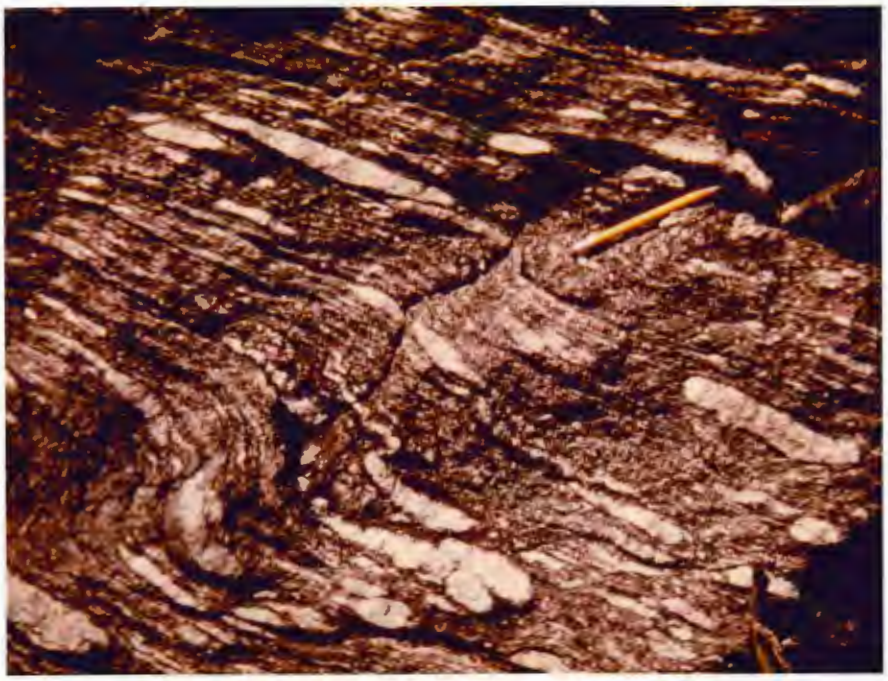

Figure 43: Fold in lenticular gneiss represents a second deformational event. (Sample location #7)

(Note: The outcrop of lenticular gneiss at this locality lies in a questionable position, and may have slumped 10-15° but this is difficult to determine as the lineation of the quartz-feldspar pebbles does follow the major northwestly trend.)

Elevation 9079, N.W. ¼, Section 35, Sample Location #28

This location is very important in that several structural features can be observed: 1) an isoclinal fold with axial planar quartz-sillimanite knots in laminated biotite-quartz-feldspar gneiss (Figure 33B), 2) dome and basin, or saddle fold, indicating two periods of deformation (Figure 39), 3) discordant granitic dike (Figure 41B), 4) amphibolite lens pinched out by laminated biotite-quartz-feldspar gneiss, and 5) very traceable, fine compositional layering in laminated biotite-quartz-feldspar gneiss.

Overlook -- located at section line between Sections 1 & 12 at Sample location #45.

The importance of this location is crucial to the structural interpretation. Here lies the only refolded isoclinal fold observed in the present study (Figure 40).

## Structural Conclusions

The structure of the Farmington Canyon Complex is complex. There exists evidence for at least three periods of deformation with certain structural data which may indicate an additional event or a later stage of one of the main events (Table 1).

The first deformational event is represented by the refolded isoclinal fold (Figure 40). A regional metamorphic event of amphibolite-grade followed about 1700 $\pm$ 150 M.Y. ago (Bryant, 1980). This event was responsible for the formation of the northwest trending mineral lineations and the tight and isoclinal folds with northwest trending fold axes. The third event, represented by southwest trending mineral lineations and fold axes, probably occurred during the Late-Precambrian, but may represent the latter stages of the amphibolite-facies metamorphic event.

Thrust faults associated with the Sevier orogeny (pre-Late Cretaceous, 80 M.Y.) are observed locally near Ogden, Utah (Bruhn and Beck, 1981). No evidence for thrust faulting was observed in the present study. However, shear zones believed to be associated with the Sevier orogeny are observed at Bountiful Peak.

A problem exists in interpreting the data on axial planar measurements. Two sets of planes exist, as previously mentioned. One possible explanation might be that one set of planes, those inclined steeply southwest, was the result of the amphibolite-facies event and the second set, those inclined moderately to the northeast, formed as a result of a minor event at the same time or shortly afterwards (Table ).

A second explanation would result from the construction of a rough girdle on the contoured stereonet (Figure 34B). This would represent folding of one initial set of folds. The result would be a fanning of axial planes about a fold axis of N. 42 W., 12 N.W. One would therefore conclude that indeed there were two periods of deformation and that they were, in fact, coaxial. If this were the case, it would just add to the structural complexity of the Farmington Canyon Complex.

Minor problems still exist. A detailed structural study over the whole Farmington Canyon Complex would hopefully enable one to fit the fine details into the broader picture discussed above.

Table I: Possible breakdown of structural data according to periods of deformation.

| EVENT | | EVIDENCE | DATE |
|---|---|---|---|
| I | A) | Refolded isoclinal fold<br>First fold axis -- N. 45 W., 35<br>Axial plane -- N. 30 E., 44 N.W. | Pre-1850 M.Y. |
| II | A) | Refolded isoclinal fold<br>Second fold axis -- N. 31 W., 10<br>Axial plane -- N. 20 W., 74 S.W. | 1700 ± 150 M.Y. (Amphibolite-facies event) |
| | B) | Lineations with northwest trend<br>1) Fold axes -- N. 51 W., 14<br>2) Mineral lineations<br>a) Quartz-sillimanite knots N. 60 W., 15-18<br>b) Elongate quartz-feldspar pods N. 54 W., 21<br>c) Biotite -- N. 36 W., 22<br>d) Hornblende -- N. 34 W., 11 | |
| | C) | Set of folds with axial planes dipping southwest<br>N. 40 W., 68 S.W. | |
| II½ | A) | Set of folds with axial planes dipping northeast<br>N. 64 W., 20 N.E. | 1700 ± 150 M.Y. or Late-PE? |
| III | A) | Folded lenticular gneiss<br>Fold axis -- S. 42 W., 40 | Late-PE? |
| | B) | Biotite lineation -- S. 60 W., 40 | |
| | C) | Dome & basin fold: superposition of second folds on folds with northwest plunging fold axes formed during event II | |
| IV | A) | Shear zones: may be a separate event or coincident with event III | Late-PE? or 80 M.Y. (Sevier Orogeny) |

## Uranium-Thorium Potential of Bountiful Ridge

A study in conjunction with the United States Department of Energy's National Uranium Resource Evaluation Program was performed to assess the favorability of Precambrian metasedimentary rocks in northern Utah for deposits of uranium in Precambrian quartz-pebble conglomerates (Graff et. al., 1980). Rocks of Early Proterozoic age that consist of thick, clastic sequences within the Uinta Arch were examined.

Rocks from the Farmington Canyon Complex considered in the Department of Energy's study are exposed two to three miles south of the present study, in the Sessions Mountains where a relatively thick, mature, clastic sequence of quartzites exists. A radiometric survey using a McPhar TV - 1A hand-held gamma-ray spectrometer was completed. KUTh values range from 1000-7000 CPM and average 2550 CPM. UTh values range from 50 to 350 CPM and average 155 CPM. A suite of samples were chemically analyzed. Two samples contained between 12-15 ppm uranium.

The present study consisted of a radiometric survey (Plate 1), using a Mount Sopris SC-131A scintillometer, and preparation of radioluxographs to detect the presence of uranium-thorium bearing minerals. Values ranged from about 100 to 850 CPS and averaged 200 to 250 CPS. Background

was approximately 175 CPS (Table II). Values over 700 CPS were considered high for this study. Two such readings, with values up to 850 CPS, were recorded in two east-west trending shear zones 40-60 feet wide, on the north slope of Bountiful Peak. These zones have already been described petrographically (p 51). The radioactive mineral is believed to be monazite and occur as flesh colored grains up to 5 mm in length.

The radioluxographs were developed with the use of a polaroid back and attachable cover called an Alfaprint-1 (Figure 44). The method utilizes Polaroid 3000 ASA Type 667 film and is relatively simple. First the rock sample is cut and ground to a 1000 mesh or polished. Radiation-sensitive scintillator paper is placed directly on the film. The polished rock slab is then placed on the scintillator paper. The Alfaprint-1 is then left undisturbed in complete darkness to expose the film. Exposures vary from several hours to two or three days. After developing, the result is a non-reversed image of the sample on a light background. Radioactive phases occur as light domains (Figure 45).

Radioluxographs were prepared for each rock type. However, only the samples from the sheared granite gave positive results (Figure 45). Light domains on the radioluxograph correspond to brown monazite grains in the polished sample. Small concentrations of monazite within the shear zones is possibly due to the processes of hydrothermal mineralization and mylonitization.

Table II: Uranium-thorium distribution along Bountiful Ridge.

| Rock unit | Value CPS | Average CPS |
|---|---|---|
| Granite | 100-250 | 200 |
| Sheared granite | 200-850* | 250 |
| Amphibolite | 90-350 | 175 |
| Migmatitic amphibolite | 300-350 | 300 |
| Granitic gneiss | 250-500 | 250 |
| Cordierite-garnet-anthophyllite gneiss | 200-250 | 225 |
| Hornblende-cummingtonite-garnet gneiss | 200 | 200 |
| Laminated biotite-quartz feldspar gneiss | 150-400 | 240 |
| Lenticular gneiss | 200 | 200 |
| Biotite-sillimanite gneiss | 200-350 | 300 |
| Heterogeneous cordierite-garnet-biotite gneiss | 210 | 210 |

Background 170-180 CPS

*North slope of Bountiful Peak

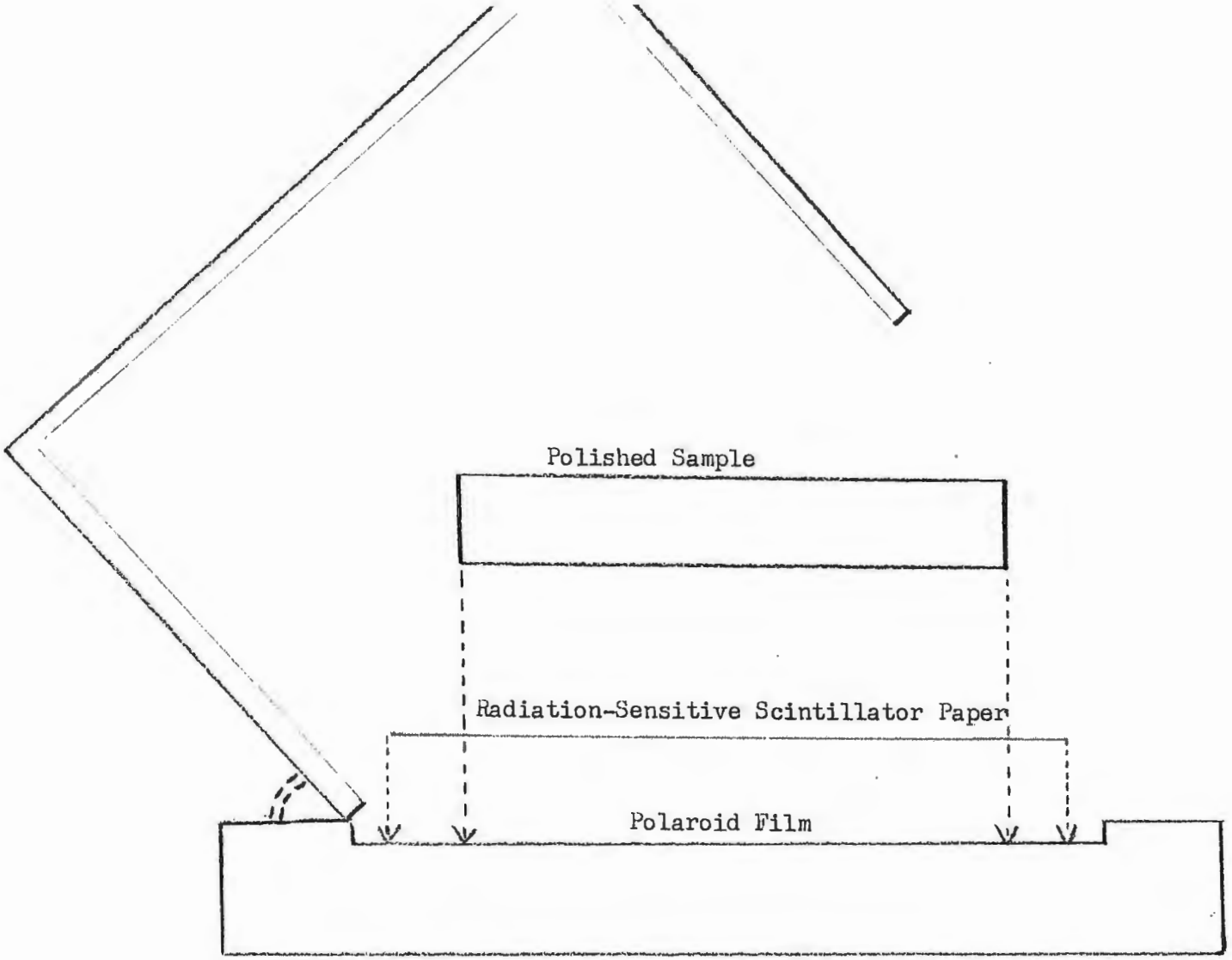


Figure 44: Method of producing a radioluxograph using the Alfaprint-1.

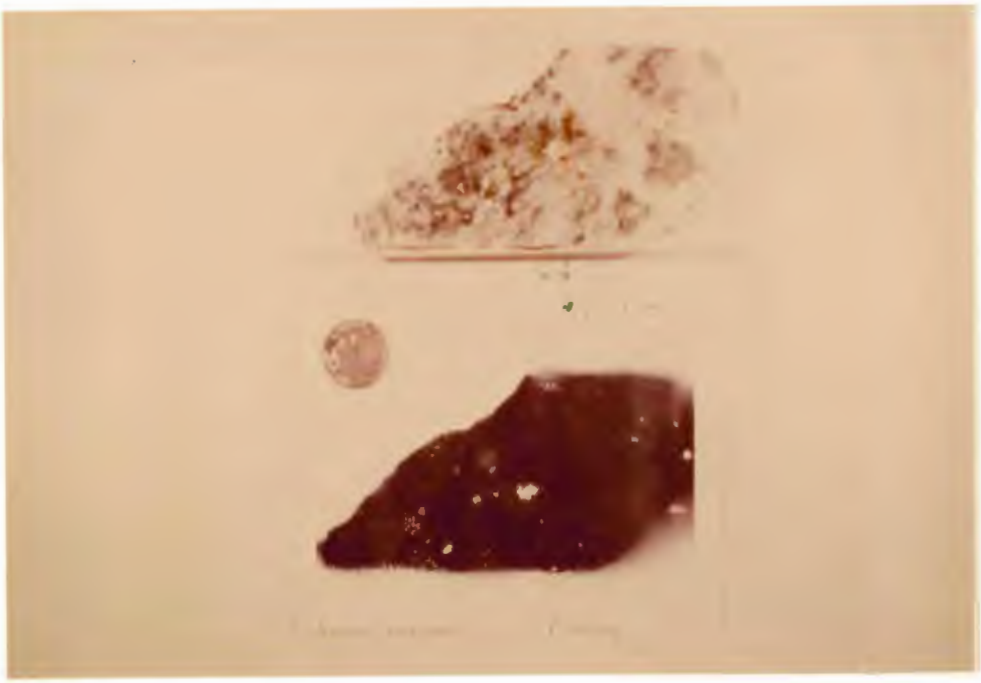

Figure 45: Polished hand sample and corresponding radioluxograph of sheared granite. Brown, radioactive mineral is monazite. Film was exposed for approximately 4 hours, 45 minutes. Location 16.

The potential for uranium occurrences in the Farmington Canyon Complex is considered poor, as no anomolies from the Department of Energy's research, or the present study were found. Conditions for uranium remobilization during high-grade metamorphism and associated igneous activity were favorable, but no evidence for uranium concentration has been observed.

## Metamorphism and Interpretation

### General Statement

Mineral assemblages within the metasedimentary and metavolcanic rocks are diagnostic of high-grade metamorphism (Winkler, 1979), specifically upper amphibolite grade (Turner, 1968). The pelitic assemblage of sillimanite-K feldspar-quartz-muscovite-plagioclase has been observed. This suggests the maximum P-T conditions of metamorphism have attained the second sillimanite isograd. Under such conditions, incipient partial melting may occur, but is unlikely to be extensive. Textural and mineralogical evidence for this will be presented.

### Maximum Pressure-Temperature Conditions of Metamorphism

The conditions of metamorphism can be determined by the use of a petrogenetic grid developed from natural and experimental data and compared graphically with coexisting mineral assemblages. By applying Schreinemakers' rules, a schematic grid (Figure 46) for pelitic rocks involving the phases K feldspar-muscovite-aluminosilicate-biotite-cordierite-garnet-orthoamphibole or orthopyroxene has been developed (Grant, 1973).

Pertinent mineral assemblages from quartz-bearing pelitic rocks are[1]: 1) QKPMBG and 2) QKPMA $\pm$ BG from the laminated biotite-quartz-feldspar gneiss; 3) QPABCG from the heterogeneous cordierite-garnet-biotite gneiss; 4) $QPBCGO_a$ from the cordierite-garnet-anthophyllite gneiss.

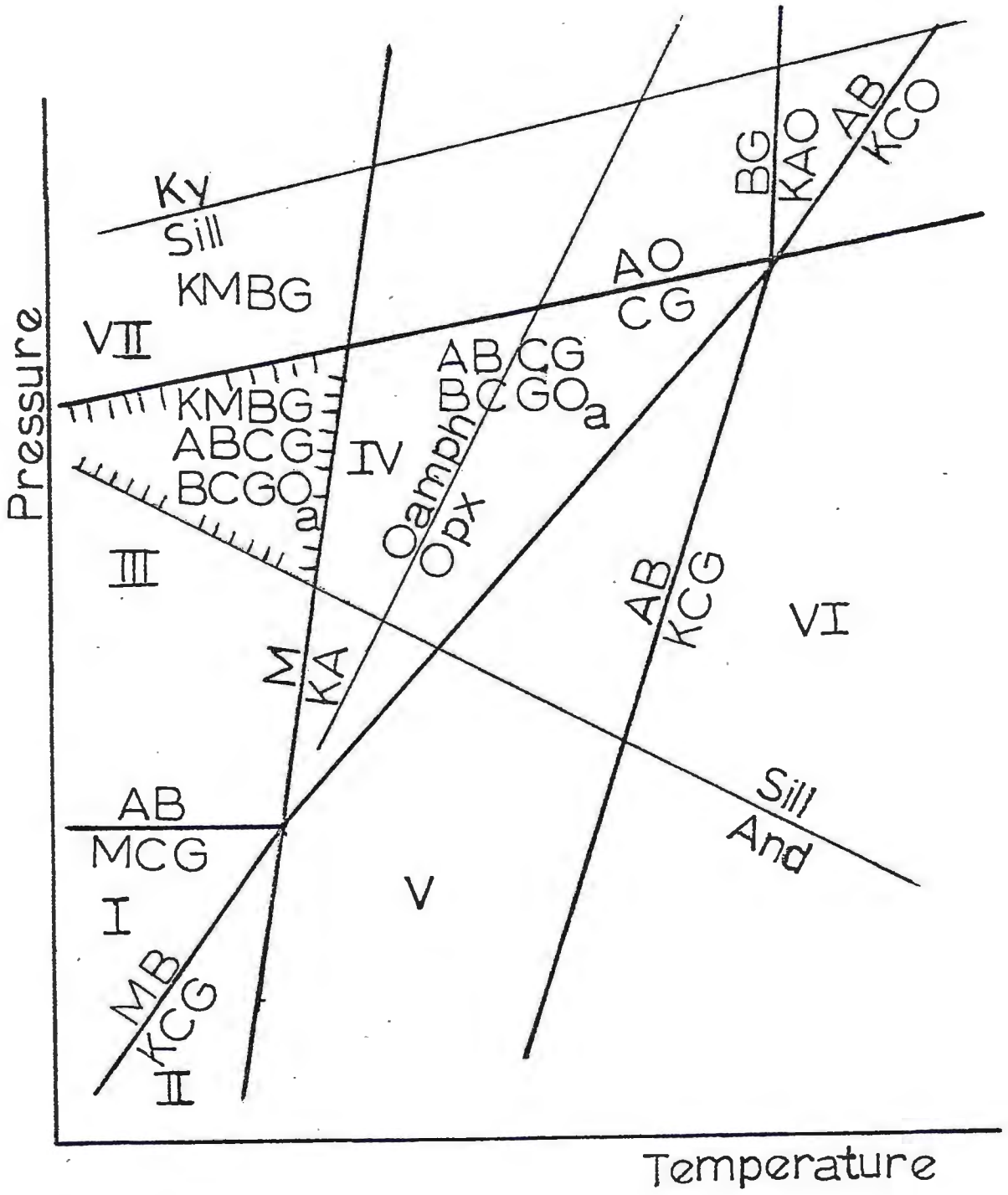


Figure 46: Schematic petrogenetic grid involving phases $KMABCGO_aO_p$ for quartz bearing pelitic rocks.

The approximate position of the aluminosilicate polymorphic transitions and of the transition between orthoamphibole and orthopyroxene bearing assemblages are shown (after Grant, 1973).

[1] Abbreviations for phases:
Q: quartz
K: potassium feldspar
P: plagioclase
Ab: albite
M: muscovite
A: aluminosilicate (sillimanite)
B: biotite
C: cordierite
G: garnet
$O_a$: orthoamphibole (anthophyllite)

---

Assemblages (3) QPABCG and (4) QPBCG$O_a$ are stable in "mini-facies" III and IV. Assemblage (1) QKPMBG is possible in "mini-facies" III and VII and assemblage (2) QKPMA ± BG is stable only on the univariant reaction QM = KAV. Under equilibrium conditions, these four assemblages are therefore stable only in "mini-facies" III.

The coexistence of sillimanite-K feldspar-muscovite-quartz ± plagioclase suggests the P-T conditions extended to the second sillimanite isograd (Evans and Guidotti, 1966). QCG is stable but sillimanite does not coexist with orthoamphibole. Sillimanite is the only aluminosilicate present which indicates that P-T conditions are on the high-temperature side of the polymorphic transition: andalusite = sillimanite. Therefore, the conditions of metamorphism are limited by the following reactions: M = KA, AO = CG, and andalusite = sillimanite.

The second sillimanite isograd is well defined (Chatterjee and Johannes, 1974) and the high pressure limit of the assemblage QCG is apparently within the sillimanite field (Grant, 1973). The andalusite-sillimanite transition is still not firmly fixed (Day and Kumin, 1980) and Holdaway (1971) and are shown on figure 47.

An estimate of the conditions of metamorphism can be determined by the use of Hensen and Green's (1973) P-T diagram of [1] $X_{Cd}$ and $X_{Ga}$ values for the divariant reaction: cordierite + hypersthene = garnet + quartz, and from Grant's (1981) microprobe data on coexisting garnet-cordierite-orthoamphibole gneiss (location 31). The P-T conditions thus determined are approximantly 630° C and 6 Kb. It must be emphasized that these values be taken as a first approximation as Hensen and Green's P-T diagram is for use with coexisting cordierite-garnet-orthopyroxene, not orthoamphibole.

Possible evidence for (and against) Partial Melting

Grant (1968) suggested that a common protolith and also a common premelting assemblage of K feldspar-plagioclase-biotite-sillimanite-quartz may give rise to a cordierite-anthophyllite bearing residuum and a granitic melt by partial melting, filter pressing and recrystallization.

---

[1] mole fraction: $X_{Ga} = \frac{Mg^{Ga}}{Mg^{Ga} + Fe + 2Ga}$

$$X_{Cd} = \frac{Mg^{Cd}}{Mg^{Cd} + Fe + 2Cd}$$

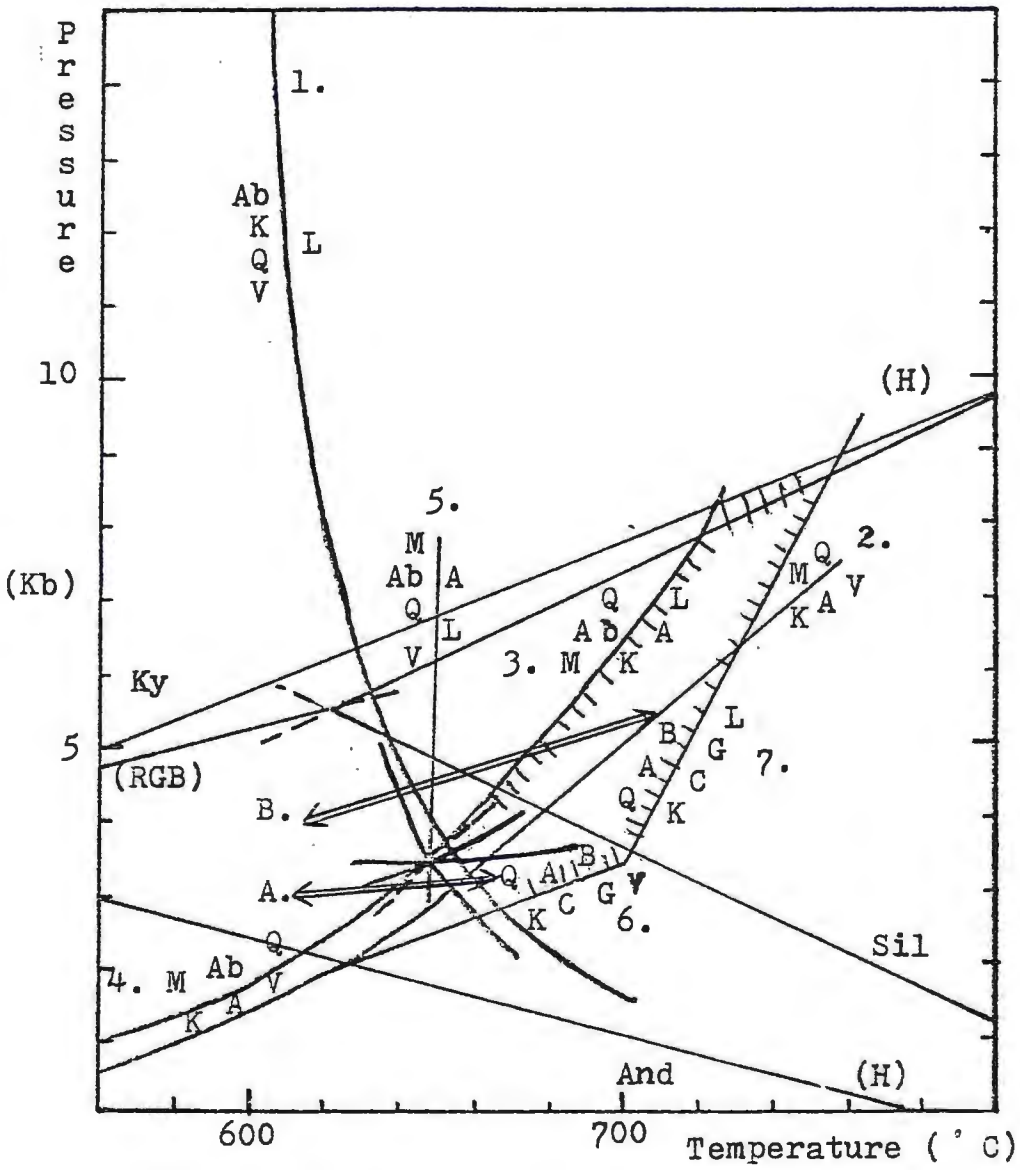


Figure 47: Petrogenetic grid, modified after Thompson and Algor (1977). $Al_2SiO_5$ phase relations from Richardson et al. (1969, RGB) and Holdaway (1971, H). The univariant curves are from the following sources: (1) Luth et al. (1964), (2) Chatterjee and Johannes (1974), (3) Peto and Thompson (1974), (4) Thompson (1974), (5) Storre and Karotke (1971), (6) and (7) Hoffer and Grant (1980).

The cordierite-garnet-anthophyllite gneiss contains assemblages of plagioclase-quartz-garnet-biotite in addition to cordierite and anthophyllite. Foliation is defined by layers of anthophyllite and associated cordierite. Cordierite commonly surrounds garnet, suggesting the cordierite formed after the development of the garnet. Anthophyllite is randomly oriented. One would expect a prismatic mineral to show a preferred orientation if the rock formed concurrently with the second major deformational event which produced several northwest trending mineral lineations (Table 1). The nonalignment of the anthophyllite also suggests late formation.

The late formation of cordierite and anthophyllite would suggest that they are products of the reaction (Grant, 1968):

Quartz + Plagioclase + Biotite + Garnet + Vapor =
Cordierite + Anthophyllite + Granitic Liquid

The reaction proposed by Grant utilized pure albite, whereas the plagioclase in the laminated biotite-quartz-feldspar gneiss is $An_{40}$. Higher temperatures would be required to initiate melting in this case because of the higher calcium content of the plagioclase.

Other possibilities might include (1) Fe-Mg metasomatism accompanying contact metamorphism (Eskola, 1914); (2) prograde metamorphism of altered mafic lavas (Vallance, 1967);

(3) prograde metamorphism of iron and magnesium rich alteration zones which underlie many volcanogenic Cu-Zn sulfide deposits (DeRosen-Spence, 1969; Chinner and Fox, 1974).

The occurrence of leucocratic veins in the migmatitic amphibolite and the heterogeneous cordierite-garnet-biotite gneiss might at first indicate formation as a result of partial melting, especially since the P-T conditions of metamorphism have reached the second sillimanite isograd. However, the composition of these veins is not granitic (composed of quartz-plagioclase-K feldspar). Rather they consist of plagioclase ($An_{55}$) and quartz. This would require liquidus temperatures in excess of 800° C at 5 Kilobars with compositions of $An_{55}$ for melting (Yoder, 1968).

The origin of migmatites has long been disputed. Other possible origins for the formation of these rocks include: metasomatic introduction of K, Na, and/or other elements to form the veins, and metamorphic differentiation (Hyndman, 1972).

Leucocratic pods within the laminated biotite-quartz-feldspar gneiss have been studied and interpreted to be a result of incipient partial melting based on mineralogical and textural evidence. The pods are typically coarse-grained and are quartzofeldspathic in composition.

The leucocratic pod shown in figure 7 consists of coarse-grained perthitic K feldspar, quartz and minor plagioclase. The K feldspar grains are broken, but in optical continuity,

and are surrounded by large grains of muscovite which are of secondary origin. No sillimanite was found in this pod.

The leucosome of sample FCB 5-15 (figure 8) consists of sillimanite prisms and needles contained within coarse-grained quartz and perthitic K feldspar. The melanosome consists of a fibrous mat of fine-grained sillimanite intergrown with biotite. Small garnet porphyroblasts are closely associated with the sillimanite-biotite intergrowth. The portion of the garnet in the pod itself is surrounded by a very thin rind (less than 0.5 mm) of optically continous K feldspar (figure 9). The rest of the garnet is enclosed by an intergrowth of sericite, sillimanite and biotite.

The occurrence of these leucocratic pods is not commonplace in the laminated biotite-quartz-feldspar gneiss. The fact that their quartzofeldspathic composition, under proper conditions, would be well suited to melting, suggests that conditions were not appropriate for broad scale partial melting. Possible explanations for this lack of partial melting include: a) sporadic distribution of or lack of water, b) temperatures too low, or c) anorthite content too high. Water could be concentrated within certain layers in a paragneiss and appreciable melting would occur only where appreciable amounts of water were present, whereas an increase in anorthite (CaO) raises the temperature required for melting.

The leucocratic pod in figure 8 may represent the best evidence for partial melting. The present assemblages in sample FCB 5-15 are QKPMAB(G) in the melanosome and QKPMAB in the leucosome. However two assumptions are made: 1) the minor muscovite is retrograde and 2) that a liquid formed at least part of the leucosome. Based on these assumptions, the assemblage at the peak of metamorphism may have been QKPABGL, assuming the liquid (L) to be of granitic composition.

The coexistence of QAB appears to be stable and there is no evidence of reaction between ABG. So the conditions of metamorphism were at least within the stability field of QAB (Figure 47). The possible relations involving the subassemblage QKPA, neglecting biotite, garnet and muscovite, should therefore be considered.

Certainly domains 2-3 mm across of QKA are present in the leucosome. Assuming the muscovite to be secondary, the assemblage QKA existed without muscovite and the second sillimanite isograd was exceeded.

Possible P-T paths within the K-Na system are shown on figure 47. The formation of QKPA may be due to 1) dehydration or low pressure, shown by path A or 2) melting or high pressure, shown by path B. The subassemblage QKPAL could be attained by either path at high temperatures. Complete recrystallization to subsolidus conditions below

the second sillimanite isograd from path A or B could give very similar products, i.e. quartz-K feldspar-aluminosilicate and retrograde muscovite. However, fibrous sillimanite is intergrown with perthitic K feldspar in the leucosome which suggests that perhaps this sillimanite was produced in association with the leucosome. The scanty evidence would therefore favor path B over A (Figure 47), in which melting would not begin in the vapor absent system, containing the assemblage QKPA, until the reaction QAbM = KAL were crossed. The effect of adding anorthite to the second sillimanite isograd reaction would be to move this reaction to higher temperatures, at constant pressure.

Based on the assumptions that muscovite is retrograde and that at least a portion of the leucosome formed from a granitic liquid, the conditions of metamorphism would then be restricted by the following reactions: MAbQ = KAV, QAB = KCGV, QAB = KCGL and Ky = Sil.

## Origin of Pegmatitic Granite and the Common Occurrence of Graphic Granite

Granitic pegmatite magma can be generated by the following means: as a rest-liquid in a cooling igneous body yielding dominantly anhydrous crystallizing phases, or as a result of partial melting of crustal materials (Jahn and Burnham, 1969).

The presence of aluminous minerals would suggest derivation from partial melting of aluminous rocks. The non-rotated biotite schlieren within the granite would further suggest a passive emplacement.

A pegmatitic magma must consist of a silicate melt that is saturated with water and/or other volatile substances. The water-saturated magma is a key condition for the genesis of pegmatites, according to the model proposed by Jahns and Burnham. This may be accomplished through fractional crystallization of dominantly anhydrous minerals, reduction of confining pressure or osmotic processes. The development of a second fluid phase, an aqueous one, occurs when the second boiling point is reached. The principal role of the aqueous liquid is to promote growth of very large crystals characteristic of pegmatites, whereas the silicate melt would produce finer-grained products.

Late stages of pegmatite development according to the model, would typically consist of varying amounts of silicate melt and aqueous liquid in the supercritical state. Crystallization would produce coarsely porphyritic to pegmatitic products. Fine-grained aplitic material could result any time there is a sudden reduction in confining pressure. This would cause a loss of dissolved liquid in the silicate melt, therefore suddenly moving the silicate melt into the subsolidus region. Quick crystallization of fine-grained aplite would necessarily follow.

Graphic granite is an intergrowth of subhedral skelatel quartz prisms in a K feldspar host (Figure 30). Quartz is crystallographically oriented relative to the feldspar host and exhibits cunieform basal outlines (Baker, 1967, 1970).

The origin of graphic granite is uncertain. Several possibilities exist, including simultaneous crystallization of quartz and K feldspar at a eutectic (Barker, 1967, Hyndman, 1972, and Carmichael, Turner and Verhoogen, 1974), and partial replacement of one mineral by the other (Hyndman, 1972, Carmichael, Turner and Verhoogen, 1974). Jahns and Burnham (1969) suggest the graphic texture might be representative of the transfer of silica, through the aqueous phase, that is not fixed in feldspar and micas.

## Dynamic Metamorphism

Zones of mylonite and thrust faults are abundant north of the present study, whereas two shear zones within the granite exist of the north slope of Bountiful Peak. These zones are recognized megascopically by a pale green mottled color, indicating a high degree of chloritization, and by the high percentage of quartz, relative to the granite.

Cataclasis is readily observed microscopically. Mortar texture is well developed in quartz. Feldspar is elongate, anhedral and completely altered to sericite and chlorite. Euhedral monazite is concentrated in small areas within the shear zones.

Evidence for cataclasis, such as mortar texture, was not typically observed in the gneissic units. Only the biotite-sillimanite gneiss showed evidence for cataclasis. Very thin, elongate quartz rods and highly fractured garnet were observed.

Protolith of the Farmington Canyon Complex

The laminated biotite-quartz-feldspar gneiss could represent a thick sequence of pyroclastic tuffs and ash flows. Another possible origin for the laminated biotite-quartz-feldspar gneiss would be aluminous sediments. Additional evidence for a volcanic origin is a thin amphibolite lens in figure 17 that is comformable to the compositional banding and probably represents a mafic flow interlayered with the laminated gneiss.

The lenticular gneiss, interbedded with the laminated biotite-quartz-feldspar gneiss, may also be of volcanic origin, representing coarser-grained projectiles, such as lapilli and small bombs, deposited locally near a felsic volcanic source.

The quartzitic gneiss apparently represents impure sandstones, reflected by the presence of feldspar in the rock. A sedimentary origin for the heterogeneous gneiss is also apparent because of the pelitic compositions.

The amphibolites were probably mafic sills, flows or dikes which were interbedded with or intruded into the laminated biotite-quartz-feldspar gneiss (Figure 17).

# SUMMARY AND CONCLUSIONS

The primary objective of this study was to determine the structural and metamorphic history of the southern portion of the Precambrian Farmington Canyon Complex. It consists of a relatively thick sequence of metasedimentary and metavolcanic rocks which are complexly deformed and have undergone upper amphibolite grade metamorphism.

The complex consists of biotite-quartz-feldspar gneisses, amphibolites, migmatites, granitic gneiss and pegmatitic granite. Mineral assemblages in the amphibolite consist of hornblende-plagioclase-biotite-garnet-quartz. Important pelitic mineral assemblages include: quartz-K feldspar-plagioclase-muscovite-biotite-garnet and quartz-K feldspar-plagioclase-muscovite-sillimanite $\pm$ biotite-garnet. These assemblages indicate that the maximum pressure-temperature conditions of metamorphism reached the second sillimanite isograd and may have exceeded it.

An Archean granulite grade metamorphic event has been documented by the presence of relict hypersthene found elsewhere within the Farmington Complex (Bryant 1980). An upper amphibolite grade metamorphic event of middle proterozoic age ($1700 \pm 150$ M.Y.) was coincident with the second major deformational event. The main mineral assemblage and northwest mineral lineations, which parallel the northwest trending folds, were formed at this time.

Dynamic metamorphism is closely associated with the thrusting and mylonitization of the Sevier Orogeny. Shear zones on the north slope of Bountiful Peak exhibit well developed mortar texture, recrystallization and are highly silicified.

Evidence for at least three periods of deformation have been observed. Rare evidence for the first event is a refolded isoclinal fold with northwest trending fold axes. The second event is recognized by the presence of mineral lineations and northwest trending fold axes. The predominance of the second event masks other structures which may be a result of the first event.

Minor evidence for a third deformational event is seen as a gentle warping associated with the superposition of a minor set of folds upon folds with northwest trending fold axes from event II. The result is the development of rare dome and basin folds. Several minor biotite lineations trending southwest are also evidence for this third event.

The fourth deformational event is characterized by thrusting and zones of mylonitization north of the study area and by shear zones on the north slope of Bountiful Peak. The thrusting and mylonitization is probably a result of the Sevier Orogeny (Bruhn and Beck, 1981). The shear zones are also thought to be related to the Sevier Orogeny.

The conclusions of this study are:

1) The Farmington Complex has undergone at least three major deformational events, and perhaps even a fourth. The predominance of the second deformational event is such that evidence for the first and third events is rare. This is perhaps the reason the complex structural history has not been satisfactorily determined.

2) Evidence for two episodes of metamorphism has been recognized, an upper amphibolite event during the middle Precambrian and a dynamic event probably during the pre-Late Cretaceous Sevier Orogeny. In addition, an archean granulite facies metamorphism was suggested by Bryant (1980).

3) Maximum P-T conditions during the amphibolite grade metamorphism extended at least up to the second sillimanite isograd and may have exceeded it. Paucity of evidence for partial melting may be due to: a) lack of water, b) anorthite content too high, and/or c) inadequate temperatures.

# BIBLIOGRAPHY

Barker, D. S., 1967, Texture, Composition and Origin of Graphic Granite (abs): Can Min., v. 9, pg 284.

_____, 1970, Composition of Granophyre, Myrmekite and Graphic Granite: Geol. Soc. Am Bull., v. 81, pg 3339-3350.

Bell, G. L., 1951, Geology of the Precambrian Metamorphic Terrane, Farmington Mountains, Utah: Ph. D. Thesis, Univ. of Utah, pg 101.

Bruhn, R. L. and Beck, S. L., 1981, Mechanics of Thrust Faulting in Crystalline Basement, Sevier Orogenic Belt, Utah: Geology, v. 9, pg 200-204.

Bryant, B., 1978, Farmington Canyon Complex, Wasatch Mts., Utah (abs.): Geol. Soc. Am. Abstr. Programs, v. 10, No. 5, pg 211, The Geol. Soc. of Am. Rocky Mt. Section, 31st Annual Meeting, Precambrian Retrograde Metamorphism.

_____, 1980, Metamorphic and Structural History of the Farmington Canyon Complex, Wasatch Mountains, Utah (abs.): Geol. Soc. Am. Abstr. Programs, v. 12, NO. 6, pg 269, The Geol. Soc. of Am. Rocky Mt. Section, 33rd Annual Meeting.

Carmichael, I. S., Turner, F. J. and Verhoogen, J., 1974, Igneous Petrology: New York, McGraw-Hill Inc., pg 739.

Chatterjee, N. D. and Johannes, W., 1964, Thermal Stability and Standard Thermodynamic Properties of Synthetic $2M_1$-Muscovite, $KAl_2AlSi_3O_{10}(OH)_2$: Contrib. Mineral. Petrol. v. 48, pg 89-114.

Chinner, G. A. and Fox, J. S., 1974, The Origin of Cordierite-Anthophyllite Rocks in the Land's End Aureole: Geol. Mag., v. 111, pg 397-408.

Damon, P. E., Gast, P. W., Hashad, A., Sayyah, T., and Whelan, L. A., 1968, Geochronology of the Precambrian of Northern Utah (abs.): Geol. Soc. Am. Spec. Paper 101, pg 394.

Day, H. W., and Kumin, H. J., 1980, Thermodynamic Analysis of the Aluminum Silicate Triple Point: Am Jour. Sci., v. 280, pg 265-287.

Deer, W. A., Howie, R. A., and Zussman, J., 1966, An Introduction to the Rock Forming Minerals: New York, John Wiley and Sons, Inc., pg 528.

DeRosen-Spence, A., 1969, Genese Des Rockes a Cordierite - Anthophyllite des Gisements Cupro-Aincifers de la Region de Rouyn-Noranda, Quebec, Canada: Can. Jour. Earth Sci., v. 6, pg 1339-1345.

Eardley. A. J., and Hatch, R. A., 1940, Precambrian Crystalline Rocks of North-Central Utah: Jour. Geol., v. 48, No. 1, pg 58-72.

Eardley, A. J., 1944, Geol. of the North-Central Wasatch Mountains, Utah: Geol. Soc. Am. Bull., v. 55, No. 7, pg 819-894.

Eskola, P., 1914, On the Petrology of the Orijarvi Region in Southwestern Finland: Comm. Geol. Finlande Bull., v. 40, pg 279.

Evans, B. W. and Guidotti, C. V., 1966, The Sillimanite-Potash Feldspar Isograd in Western Maine, USA: Contr. Mineral. Petrol., v. 12, pg 25-62.

Graff, P. J., Sears, J. W. and Holden. G. S., 1980, The Uinta Arch Project -- Investigations of Uranium Potential in Precambrian X and Older Metasedimentary Rocks in the Uinta and Wasatch Ranges, Utah and Colorado: Research Associates of Wyoming, Prepared for US Department of Energy.

Grant, J. A., 1968, Partial Melting of Rocks as a Possible Source of Cordierite-Anthophyllite Bearing Assemblages: Am. J. Sci., v. 266, pg 908-931.

_____, 1973, Phase Equilibria in High-Grade Metamorphism and Partial Melting of Pelitic Rocks: Am. J. Sci., v. 273, No. 4, pg 289-317.

_____, 1981, in press, Orthoamphibole and Orthopyroxene Relations in High-Grade Metamorphism of Pelite Rocks: Am. Jour. of Sci.

Hensen, B. J., and Green, D. H., 1973, Experimental Study of the Stability of Cordierite and Garnet in Pelitic Compositions at High Pressures and Temperatures III. Synthesis of Experimental Data and Geological Applications: Contr. Mineral. and Petrol., v. 38, pg 151-166.

Hintze, Lehi F., 1973, Geologic History of Utah: Brigham Young University Geology Studies, v. 20, part 3.

Hoffer, E. and Grant, J. A., 1980, Experimental Investigation of the Formation of Cordierite-Orthopyroxene Parageneses in Pelitic Rocks: Contrib. Mineral. Petrol., v. 73, pg 15-22.

Holdway M. J., 1971, Stability of Andalusite and the Aluminum Silicate Phase Diagram: Am. Jour. Sci., v. 271, pg 97-131.

Hyndman, D. W., 1972, Petrology of Igneous and Metamorphic Rocks: New York, McGraw-Hill Inc., pg 533.

Jahns, F. H. and Burnham, C. W., 1969, Experimental Studies of Pegmatitic Genesis: I. A Model for the Derivation and Crystallization of Granitic Pegmatites: Econ. Geol. v. 64, pg 843-864.

Kerr, Paul F., 1977, Optical Mineralogy: New York, McGraw-Hill, Inc., pg 492.

King, P. B., 1977, Precambrian Geology of the United States; An Explanatory Text to Accompany the Geologic Map of the United States: Geologic Survey Professional Paper 902, pg 85.

Luth, W. C., Jahns, R. H. and Tuttle, O. F., 1964, The Granite System at Pressures of 4 to 10 Kilobars: J. Geophys. Res., v. 69, pg 759-773.

Petö, P. and Thompson, A. B., 1974, Wet and Dry Melting of White Mica-Alkali Feldspar Assemblages (Abs.): Trans. Am. Geophys. Union, v. 55, pg 479.

Ragan, D. M., 1973, Structural Geology: An Introduction to Geometrical Techniques: New York, John Wiley and Sons, pg 208.

Ramsay, John G., 1967, Folding and Fracturing of Rocks: New York, McGraw-Hill, Inc., pg 568.

Richardson. S. W.. Gilbert, M. C., and Bell, P. M., 1969, Experimental Determination of Kyanite-Andalusite and Andalusite-Sillimanite Equilibria: the Aluminum Silicate Triple Point: Am. Jour. Sci., v. 267, pg 259-272.

Storre, B. and Karotke, E., 1971, in Winkler, 1979: Fortschr. Mineral.. v. 49, pg 56-58.

Thompson, A. B., 1974, Calculation of Muscovite-Paragonite-Alkali Feldspar Phase Relations: Contrib. Mineral. Petrol., v. 44, pg 173-194.

Thompson, A. B., 1976, Mineral Reactions in Pelitic Rocks: II. Calculation of Some P-T-X (Fe-Me) Phase Relations: Am. Jour. Sci., v. 276, pg 425-454.

Thompson, A. B. and Algor, J. R., 1977, Model Systems for Anatexis of Pelitic Rocks I. Theory of Melting Reactions in the System $KAlO_2$-$NaAlO_2$-$Al_2O_3$-$SiO_2$-$H_2O$: Contrib. Mineral. Petrol., v. 63, pg 247-269.

Thompson, J. B., Jr., 1955, The Graphical Analysis of Mineral Assemblages in Pelitic Schists: Am. Mineralogist, v. 42, pg 842-858.

Turner. F. J., 1968, Metamorphic Petrology: Mineralogical and Field Aspects: New York, McGraw-Hill, Inc., pg 403.

Vallance. T. G., 1967, Mafic Rock Alteration and Isochemical Development of Some Cordierite-Anthophyllite Rocks: Jour. Petrology, V. 8, pg 84-96.

Whelan. J. A., 1969, Geochronology of Some Utah Rocks: Utah Geol. Mineral. Survey Bull., v. 82, pg 97-104.

_____, 1970, (Ed), Radioactive and Isotopic Age Determination of Utah Rocks: Utah Geol. Mineral. Survey Bull., 81, pg 75.

Winkler. H. G. F., 1979, Petrogenesis of Metamorphic Rocks (5th ed.): New York, Springer-Verlag, pg 348.

Yoder. H. S., 1968, Carnegie Inst. Year Book, v. 66, pg 477-478.